Verónica Lee Weng

Licenciada em Química Aplicada

Corn arabinoxylan biopolymers as materials for biodegradable films for food packaging

Dissertação para obtenção do Grau de Mestre em
Química Bioorgânica

Orientador: Carla Maria Carvalho Gil Brazinha de Barros Ferreira, Investigadora, Faculdade de Ciências e Tecnologia, Universidade Nova de Lisboa

Co-orientador: Isabel Maria Rôla Coelhoso, Prof. Auxiliar com Agregação, Faculdade de Ciências e Tecnologia, Universidade Nova de Lisboa

FACULDADE DE
CIÊNCIAS E TECNOLOGIA
UNIVERSIDADE NOVA DE LISBOA

Novembro, 2020

Corn arabinoxylan biopolymers as materials for biodegradable films for food packaging

Copyright © Verónica Lee Weng, Faculdade de Ciências e Tecnologia, Universidade Nova de Lisboa.

A Faculdade de Ciências e Tecnologia e a Universidade Nova de Lisboa têm o direito, perpétuo e sem limites geográficos, de arquivar e publicar esta dissertação através de exemplares impressos reproduzidos em papel ou de forma digital, ou por qualquer outro meio conhecido ou que venha a ser inventado, e de a divulgar através de repositórios científicos e de admitir a sua cópia e distribuição com objetivos educacionais ou de investigação, não comerciais, desde que seja dado crédito ao autor e editor.

2020

Thanks to

I would like to express my gratitude to some special people that allowed me reach where I am today and conclude this challenge in a few words.

Firstly I would like to thank my advisors: Doctor Carla Brazinha, Prof. Isabel Coelhoso and Prof. Vítor Alves who received me very warmly, guided and supported me during all this journey. And Maria Serra who helped me in my first steps in this project, for having the patience and availability to teach me.

To the people that I had the pleasure to meet and befriend during this last year. Filipa Pires, thank you for all the good laughs and stories, we didn't spend much time together, but it was enjoyable every time. Mafalda Cadima, for all the support and advice from day 1 and thank you for a lot of good memories. Marisa Cardoso, thank you for all the fun car rides and moments, I was able to learn a lot with you in such a short amount of time, for listening to my concerns every time and thank you for being who you are.

To my friend Rodrigo Eduardo, who I know I can always count on, for listening, for hanging out on my boba afternoons, for making me laugh at random things. Thank you for being you, I hope we can hang out again soon.

To all the amazing people that I met in bangtansubs, who always work hard and inspire me to do too. For allowing me to meet my friend Laura, though you're far away, thank you for always be willing to listen to my rants, gaming with me or just hang out, for providing me with cute Luna pics all the time and lovely care packages. I hope we can meet soon.

To my also quite but not so quite far away friend Daniela, for checking on me from time to time, it's always fun to have our little chats. Though it didn't go as planned this year, I hope we can meet again soon

And lastly, but not least to my family, who always supported my choices, for the patience and for understanding, for raising me to be the person that I am today.

For every person I met until today, I may not have mentioned you and we may not pass or talk to each other again but thank you for changing my way to see the world and allowing me to learn from you.

I'm sorry that my words can't fulfill everything I really want to say, but once again Thank You.

I hope your spring day comes again soon.

Abstract

Corn fiber is a by-product of the starch industry, currently used as animal feed. It contains in its composition arabinoxylan, with film-forming properties, thus this material has a great interest in being valorized.

Arabinoxylan was extracted with an alkaline solution and centrifuged. The resulting extract was purified with an ultrafiltration membrane hollow-fiber unit, in a continuous diafiltration process, at two different Reynolds number at the feed side (129 and 267), under controlled temperature and permeate flux conditions. At the final diavolume of 10, rejections were higher at Reynolds number 267, (91±2)% of NaCl equivalents, $NaCl_{eq}$, and (97±1)% of ferulic acid equivalents, FA_{eq}, than at Reynolds number 129, where rejections were (87±3)% and (95±1)% of $NaCl_{eq}$ and of FA_{eq}, respectively. At both Reynolds numbers, the removal of small compounds was similar (97.0±0.3)% in $NaCl_{eq}$ and (91±1)% in FA_{eq}, meaning that the final extracts had a similar quality.

The discoloration of the purified extract was then evaluated with activated charcoal and hydrogen peroxide treatments, in which only the latter resulted in a lighter colored solution. Various formulations were applied to the decolorized extract: glycerol was used as a plasticizer and different non-hazardous diacids (succinic, malonic and citric acids) were used as cross-linkers.

The resulting films were characterized in terms of their antioxidant properties, solubility in water and mechanical properties. It was found that a decolorized film formulated with glycerol and citric acid had a lower antioxidant activity (0.053±0.001)μmol Trolox/mg film than a pure arabinoxylan film (0.091±0.002)μmol Trolox/mg film. Films were still very soluble in water, with the minimum solubility being around 70%. The decolorized film with glycerol and citric acid showed the highest tension of perforation (1.28±0.14)MPa and deformation (6.4±1.7)%.

Keywords: Corn Fiber; Arabinoxylan; Diafiltration; Biopolymer discoloration; Arabinoxylan Films

Resumo

A fibra de milho é um subproduto da indústria do amido e é atualmente utilizada como alimentação animal. Contêm na sua composição arabinoxilano, com propriedades de formação de películas, portanto este material tem grande interesse em ser valorizado.

Arabinoxilano foi extraído com uma solução alcalina e centrifugado. O extrato resultante foi purificado por ultrafiltração numa unidade membranar de fibras ocas, num processo de diafiltração contínua, a dois números de Reynolds diferentes na alimentação (129 e 267), com condições de temperatura e fluxo de permeado controlados. No diavolume final de 10, a rejeição era maior no número de Reynolds de 267, (91±2)% em equivalentes de NaCl, $NaCl_{eq}$, e (97±1)% em equivalentes de ácido ferúlico, FA_{eq}, do que a número de Reynolds de 129, onde rejeições eram (87±3)% e (95±1)% em $NaCl_{eq}$ e FA_{eq}, respetivamente. Nos dois números de Reynolds, a remoção de pequenos contaminantes foi semelhante (97.0±0.3)% em $NaCl_{eq}$ e (91±1)% em FA_{eq} o que significa que os extratos finais tinham uma qualidade semelhante.

A descoloração do extrato purificado foi testada usando tratamentos com carvão ativado e peróxido de hidrogénio, nos quais apenas esta última resultou numa solução mais clara. Várias formulações foram aplicadas ao extrato descolorado: glicerol como plasticizante e diferentes diácidos não prejudiciais (sucínico, malónico e cítrico) como reticulantes.

As películas resultantes foram caracterizadas em termos de propriedades antioxidantes, solubilidade em água e propriedades mecânicas. Uma película descolorada e formulada com glicerol e acido cítrico obteve uma atividade antioxidante inferior (0.053±0.001)µmol Trolox/mg película do que uma pelicula de arabinoxilano pura (0.091±0.002)µmol Trolox/mg película. As películas ainda eram muito solúveis em água, com um mínimo de solubilidade de cerca de 70%. A película descolorada e com glicerol e acido cítrico apresentou a maior tensão de perfuração (1.28±0.14)MPa e deformação (6.4±1.7)%.

Palavras-chave: Fibra de milho; Arabinoxilano; Diafiltração; Descoloração de biopolímero; Peliculas de arabinoxilano

Table of Contents

1. Introduction 1
    1.1 Petroleum-based and biobased polymers 1
    1.2 Hemicellulose and its film-forming ability 4
        1.2.1 Hemicellulose and Xylan 4
        1.2.2 Natural based films 4
    1.3 Arabinoxylan as resource 5
        1.3.1 Arabinoxylan 5
        1.3.2 Corn bran and corn fiber 7
        1.3.3 Arabinoxylan applications 8
        1.3.4 Extraction and Purification of Arabinoxylan 9
    1.4 Separation processes 10
        1.4.1 Types of separation 10
        1.4.2 Membranes 11
        1.4.3 Membrane processes 11
        1.4.4 Membrane transport/Mechanism of permeation 14
        1.4.5 Parameters of membrane processes 16
        1.4.6 Types of membrane configuration 16
        1.4.7 Operation modes 17
    1.5 Thesis outline and objectives 17
2. Materials and Methods 19
    2.1 Materials 19
    2.2 Extraction of Arabinoxylan 19
    2.3 Purification of the extract 19
        2.3.1 Diafiltration with hollow-fiber membrane contactor 19
        2.3.2 Operation conditions 20
    2.4 Characterization of the extract 21
        2.4.1 Determination of viscosity 21
        2.4.2 Quantification of salts present in solution 21
        2.4.3 Quantification of phenolic compounds in solution 21
        2.4.4 Determination of dry weight (total) and ashes 21

2.4.5 Determination of molecular weight by Gel Permeation Chromatography/Size Exclusion Chromatography (GPC/SEC) 22

2.5 Preservation of the purified extract 22

2.6 Decolorization of the purified extract 22

2.7 Preparation of film solution 23

2.8 Characterization of the films 23

2.8.1 Thickness 23

2.8.2 Solubility 23

2.8.3 Water Content 23

2.8.4 Color Measurement 24

2.8.5 Antioxidant Activity by Ferric Reduction Antioxidant Power (FRAP) method . 25

2.8.6 Tensile Tests (Perforation) 25

3. Results and Discussion 27

3.1 Viscosity 27

3.2 Purification Process 27

3.2.1 Purification of the diluted raw material by dia-ultrafiltration 27

3.2.2 Dry weight (total) and ashes 30

3.2.3 Molecular weight 30

3.3 Decolorization of the arabinoxylan extract 31

3.3.1 Activated charcoal adsorption method 31

3.3.2 Hydrogen Peroxide method 33

3.3.3 Optimization of decolorization method 35

3.4 Film-forming solutions and resulting films 36

3.5 Films characterization 39

3.5.1 Color Measurement 39

3.5.2 Antioxidant activity 42

3.5.3 Solubility 43

3.5.4 Mechanical tests (Perforation) 44

4. Conclusions 47

5. Future Work 49

6. References 51

7. Appendix 55

List of Figures

Figure 1.1: Chemical structure of ethylene (left) and polyethylene (right). 1

Figure 1.2: Chemical structure of propylene (left) and polypropylene (right). 1

Figure 1.3: Chemical structure of terephthalic acid (left), ethylene glycol (middle) and PET (Polyethylene terephthalate) (right). 2

Figure 1.4: Chemical Structure of styrene (left) and Polystyrene (right). 2

Figure 1.5: Chemical Structure of vinyl chloride (left) and polyvinyl chloride (right). 2

Figure 1.6: Chemical structure of a diamine (left), a dicarboxylic acid (middle) and a polyamide (right). 2

Figure 1.7: Summary of the different biodegradable biobased polymers. (source: (Haugaard *et al.*, 2000)) 3

Figure 1.8: Chemical structure of different polycarboxylic acids. 5

Figure 1.9: Chemical structure of different polyols. 5

Figure 1.10: (a) Representation of the chemical structure of arabinoxylan and its linkages (b) Possible arabinose substituents present in the arabinoxylan chain. (source: (Mendez-Encinas *et al.*, 2018)) 6

Figure 1.11: The various components that form a corn kernel. (source: (Association, 2020)) 7

Figure 1.12: Various possible separation processes according to different factors and their respective range of separation. (source: (Cheryan, 1998)) 11

Figure 1.13: Basic principle of a separation process (left), example of a setting of a membrane process (right). (source: (Mulder, 1997; Cheryan, 1998)) 12

Figure 1.14:Components that each membrane separation is usually able to split up. (source: (Cheryan, 1998)) 13

Figure 1.15: Membrane processes according to the size of the component. (source: (Cheryan, 1998)) 14

Figure 1.16: Pore diameter of each membrane process. (source: (Mohanty and Purkait, 2011)) 14

Figure 1.17: Different mechanisms of permeation: pore-flow (left) and solution-diffusion (right). (source: (Mohanty and Purkait, 2011)) 15

Figure 1.18: Different membrane processes and their respective mechanism of permeation. (source: (Mohanty and Purkait, 2011)) 15

Figure 2.1: Setting of the diafiltration process employed in this work. 20

Figure 2.2: Freeze dried purified extract. 22

Figure 2.3: Scheme of CIELAB color system. (source: (Ly *et al.*, 2020)) 24

Figure 2.4: Scheme of a perforation test. 26

Figure 3.1: Apparent viscosity (Pa.s) in function of shear rate (s^{-1}) of the different dilution of raw extract. 27

Figure 3.2: Rejection (%) in function of diavolume in equivalents of NaCl. 28

Figure 3.3: Rejection (%) in function of diavolume in equivalentes of FA. 29

Figure 3.4: Removal (%) in function of diavolume in equivalents of NaCl. 29

Figure 3.5: Removal (%) in function of diavolume in equivalents of FA. 30

Figure 3.6: Overlap of absorbance spectrum of arabinoxylan with 0.5% (w/v) of activated charcoal before (blue) and after 1h of contact (orange) in a dilution rate of 1:200. 31

Figure 3.7: Overlap of absorbance spectrum of arabinoxylan with 2% (w/v) of activated charcoal before (blue) and after 1h of contact (orange) in a dilution rate of 1:200. 32

Figure 3.8: Solution of arabinoxylan before the addition of activated charcoal (left) and filtered after the reaction time of 1h (right). 32

Figure 3.9: Overlap of absorbance spectrum of arabinoxylan with 2% (w/v) of activated charcoal before (blue) and after 24h of contact (orange) in a dilution rate of 1:200. 33

Figure 3.10: Overlap of absorbance spectrum of arabinoxylan 0.8% (w/v) with 10% (v/v_{final}) of hydrogen peroxide before (blue) and after 2h of reaction time at 45ºC (orange) in a dilution rate of 1:50. 33

Figure 3.11: Overlap of absorbance spectrum of arabinoxylan 2% (w/v) with 10% (v/v_{final}) of hydrogen peroxide before (blue) and after 2h of reaction time at 45ºC (orange) in a dilution rate of 1:100. 34

Figure 3.12: Solution of arabinoxylan before the addition of hydrogen peroxide (left) and after the reaction time of 2h at 45ºC (right). 34

Figure 3.13: Overlap of absorbance spectrum of arabinoxylan 2% (w/v) with 20% (v/v_{final}) of hydrogen peroxide before (blue) and after 2h of reaction time at 45ºC (orange) in a dilution rate of 1:200. 35

Figure 3.14: Overlap of absorbance spectrum of arabinoxylan 2% (w/v) with 10% (v/v_{final}) of hydrogen peroxide before (blue) and after 5h30 of reaction time at 45ºC (orange) in a dilution rate of 1:200. 35

Figure 3.15: Position of each arabinoxylan film in the CIELAB color circle. 41

Figure 3.16: Antioxidant activity (μmol/mg film) of film samples 1, 2 and 7 in Trolox equivalents 42

Figure 3.17: Solubility (%) of every film sample 43

Figure 3.18: Tension of perforation (MPa) of film samples tested 45

Figure 3.19: Deformation in perforation (%) of film samples tested 46

Figure A.1: Calibration curve of conductivity in function of concentration of NaCl (a)for lower concentrations (b)for higher concentrations 55

Figure A.2: Calibration curve of absorbance at 280nm in function of concentration of FA 56

Figure A.3: Calibration curve of absorbance at 595nm in function of concentration of Trolox 56

Figure A.4: Chromatogram of raw extract 57

Figure A.5:Chromatogram of purified extract 58

Figure A.6: Absorbance spectrum of hydrogen peroxide in a dilution rate of 1:200 58

List of Tables

Table 1.1: Composition of corn barn compared to corn fiber in g/kg. (source: (Rose, Inglett and Liu, 2010)) 8

Table 1.2: Different separation processes according to physical/chemical properties of the components. (adapted from: (Mulder, 1997)) 10

Table 3.1: Table of conditions of operation (Temperature (ºC), Hydraulic permeability loss (%), TMP (bar), J_{perm} ($L \cdot h^{-1} \cdot m^{-2}$) and average permeability ($L \cdot h^{-1} \cdot m^{-2} \cdot bar^{-1}$)) at Reynolds of 129 and 267 28

Table 3.2: Table of total dry weight and ashes (mg/mL) of raw extract and purified extract. 30

Table 3.3: Table of retention time (RT) at peak (min), average molecular weight at peak (Mp, kDa), average molecular weight in number (Mn, kDa), average molecular weight in weight (Mw, kDa) and polydispersity (Mw/Mn or PD) of raw and purified extract at each peak. 31

Table 3.4: Every different formulation tested of arabinoxylan films. For the decolorization process it was used hydrogen peroxide 10%(v/vfinal) for 2h at 45ºC. 36

Table 3.5: Arabinoxylan formulation and their respective obtained film. 37

Table 3.6: Values of lightness (L*), chromaticity coordinates (a* and b*) and their respective calculated hue (hº) and chroma (C*) of each arabinoxylan film. 40

Table 3.7: Values of lightness (L*), chromaticity coordinates (a* and b*) and their respective calculated hue (hº) (C*) of arabinoxylan film obtained in (Serra *et al.*, 2020). 41

Table 3.8: Color difference between a not decolorized film (1) and a decolorized one (3) and between a decolorized one (7) and a heat treated one (10). 42

Table 3.9: Thickness (mm) and Water Content (%) of film samples prepared for perforation tests 44

List of Abbreviations

Ax - Arabinoxylan

EFSA - European Food Safety Authority

FA - Ferulic Acid

FDA - Food and Drug Administration

FRAP - Ferric reduction Antioxidant Power

H2O2 - Hydrogen Peroxide

HCl - Hydrochloric Acid

HDPE - High-density Polyethylene

LDPE - Low-density Polyethylene

NaAc - Sodium Acetate

NaCl - Sodium Chloride

NaOH - Sodium Hydroxide

PA - Polyamide

PE - Polyethylene

PET - Polyethylene Terephthalate

PP - Polypropylene

PS - Polystyrene

PVC - Polyvinyl Chloride

TMP - Transmembrane Pressure

TPTZ - 2,3,5-triphenyltetrazolium chloride

1. Introduction

1.1 Petroleum-based and biobased polymers

Petroleum-based plastics have emerged in the 20th century and started to become predominant worldwide since then, especially due to their favorable physical and chemical properties and low-cost production. (Chiellini, 2008; Pereira *et al.*, 2017)

These plastics are mainly comprised of synthetic polymers (70-99%) and a smaller percentage of additives (plasticizers, antioxidants, pigments and others), usually added to provide or increase certain functionality. For food packaging purposes, every component used for the final product must be approved by health and safety authorities (for example, EFSA in Europe and FDA in USA), due to their chemical and potential toxicological properties. (Piergiovanni and Limbo, 2013)

The molecular weight of synthetic polymers usually ranges between 50-200kDa, however it's also common for a polymer to have a wider range of molecular weights, since the polymerization process may create polymer chains with different lengths. To maintain their structure, intermolecular forces are often found between chains, these interactions can vary from weak dispersion forces to strong dipole-dipole interactions. Both characteristics mentioned contribute to the physical properties of the polymer. (Piergiovanni and Limbo, 2013)

Some important and abundant polymers, nowadays, include polyethylene (PE), polypropylene (PP), polyethylene terephthalate (PET), polystyrene (PS), polyvinyl chloride (PVC) and polyamide (PA).

Polyethylene (PE) has as monomer the simplest alkene, ethylene (Figure 1.1). It's polymerized by an addition mechanism, where monomers are linked by an electrophilic addition due to the double bond. The reaction requires an initiator that forms a reactive intermediate (radical) of the monomer, which will react with other monomers (non-radical) and trigger a chain reaction. Depending on the conditions the length of the reaction can be altered, originating different products. In this case, they are separated as high-density polyethylene (HDPE: stronger, with better tensile strength and hardness) and low-density polyethylene (LDPE: soft, flexible and stretchable). (Piergiovanni and Limbo, 2013)

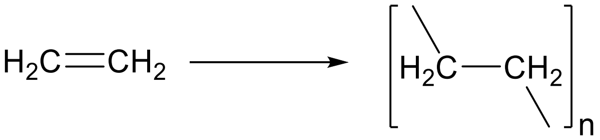

Figure 1.1: Chemical structure of ethylene (left) and polyethylene (right).

Polypropylene (PP) has a polymerization mechanism similar to the polyethylene since its monomer (propylene) only differs with the addition of a methyl group (Figure 1.2). The polymers chain can be oriented (uniaxially or biaxially) or non-oriented. Oriented films show good strength, stiffness, and gas barrier properties. (Piergiovanni and Limbo, 2013)

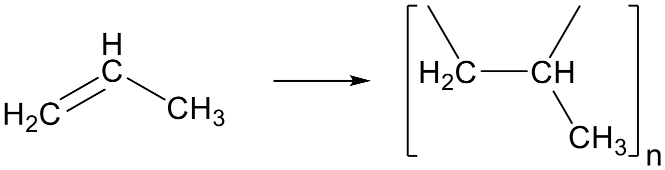

Figure 1.2: Chemical structure of propylene (left) and polypropylene (right).

Polyethylene Terephthalate (PET) has as monomers terephthalic acid and ethylene glycol (Figure 1.3), both monomers have two reactive ends allowing the formation of this polymer by a condensation reaction, where the monomers react with the removal of a water molecule. PET is a semi-crystalline polymer, that depending on the desired product can be amorphous (very transparent) or crystallized (opaque and more heat resistant). It can also be biaxially oriented or non-oriented. (Piergiovanni and Limbo, 2013)

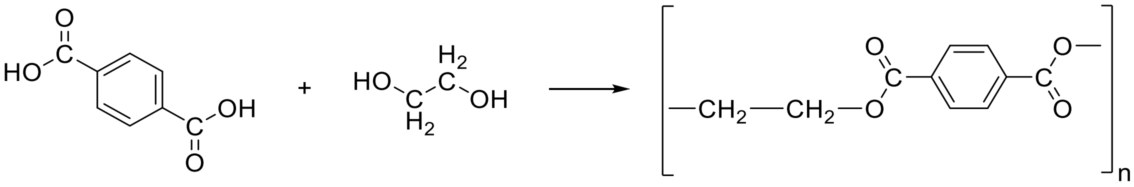

Figure 1.3: Chemical structure of terephthalic acid (left), ethylene glycol (middle) and PET (Polyethylene terephthalate) (right).

Polystyrene (PS) results from the polymerization of styrene (Figure 1.4), presenting itself usually as amorphous and clear. It has low gas barrier properties, intermediate water vapor barrier properties, low impact strength and it’s hard, yet still quite fragile. (Piergiovanni and Limbo, 2013)

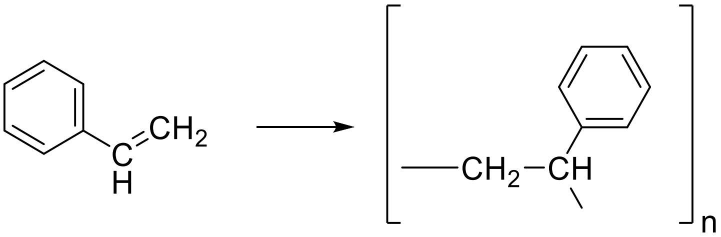

Figure 1.4: Chemical Structure of styrene (left) and Polystyrene (right).

Polyvinyl chloride (PVC) is obtained by the polymerization of vinyl chloride (Figure 1.5), since this monomer is highly carcinogenic, the polymer is carefully checked for any residual monomer. The polymer is clear, rigid and has poor thermal processing stability, therefore the addition of plasticizers is common to acquire certain desired properties. (B5)

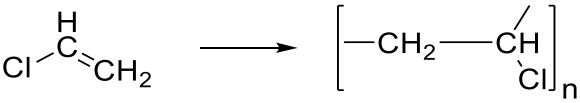

Figure 1.5: Chemical Structure of vinyl chloride (left) and polyvinyl chloride (right).

Polyamide (PA) is prepared by reacting a dicarboxylic acid with a diamine (Figure 1.6) by a condensation type of polymerization. Depending on the chain length of the monomers the polyamide has different names (for example, PA 6.6 is obtained by reacting adipic acid (C6) with hexamethylenediamine (C6)). The properties of the polymer may also vary depending on the monomers used, however, polyamides are usually good gas barriers, heat resistant and resistant to puncture. (Piergiovanni and Limbo, 2013)

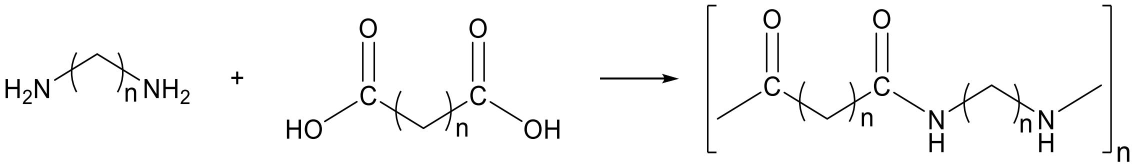

Figure 1.6: Chemical structure of a diamine (left), a dicarboxylic acid (middle) and a polyamide (right).

Nevertheless, all the polymers above mentioned are non-renewable and not biodegradable, bringing negative environmental impacts. This concern increased greatly at the beginning of the 21st century, bringing up discussions related to searching for alternative resources. (Chiellini, 2008; Pereira *et al.*, 2017)

In recent years, there's been an increase of research interest on the use of natural, biobased, renewable resources to produce biopolymers, or bioplastics, which may be biodegradable or not. (Piergiovanni and Limbo, 2013) Biopolymers, bioplastics or biobased polymers may be used, for example, as packaging (films and coatings). (Kayserilioğlu *et al.*, 2003)

Biobased polymers can be separated into three categories (Figure 1.7): (Haugaard *et al.*, 2000; Chiellini, 2008)

Category 1: polymers are directly extracted from biomass (polysaccharides like starch and cellulose or protein from plants or animals)

Category 2: polymers obtained by synthesis using biobased monomers (polylactic acid is a biopolyester constituted by lactic acid monomers, from fermentation)

Category 3: polymers produced by natural or genetically modified microorganisms (polyhydroxyalkonoates are found in many bacteria as energy and carbon resource)

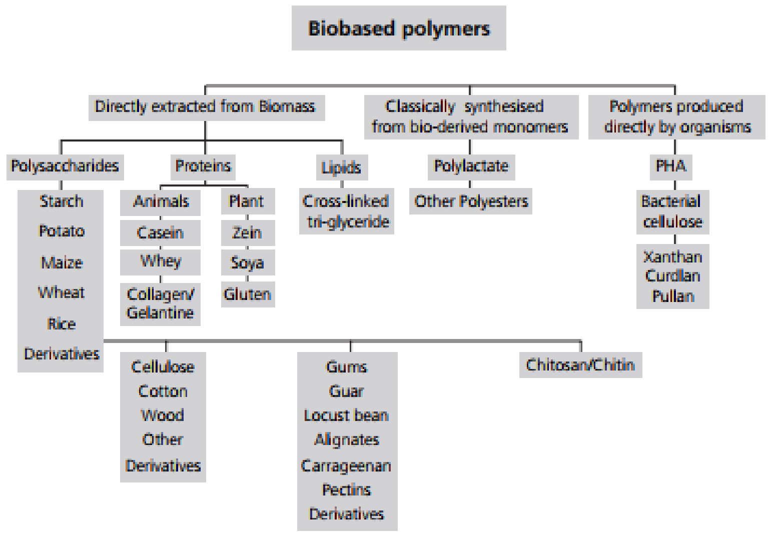
Biobased polymers
Directly extracted from Biomass
Classically synthesised from bio-derived monomers
Polymers produced directly by organisms
Polysaccharides
Proteins
Lipids
Polylactate
PHA
Starch
Potato
Maize
Wheat
Rice
Derivatives
Animals
Casein
Whey
Collagen/ Gelantine
Plant
Zein
Soya
Gluten
Cross-linked tri-glyceride
Other Polyesters
Bacterial cellulose
Xanthan
Curdlan
Pullan
Cellulose
Cotton
Wood
Other
Derivatives
Gums
Guar
Locust bean
Alignates
Carrageenan
Pectins
Derivatives
Chitosan/Chitin

Figure 1.7: Summary of the different biodegradable biobased polymers. (source: (Haugaard *et al.*, 2000))

It is believed that these biobased and biodegradable products will have a lower environmental impact than their petroleum-based and non-biodegradable counterparts. (Chiellini, 2008) Therefore, the possibility to replace the latter with natural-based packaging/materials is very attractive.

This effort can be found in various commercially available packing materials, such as the ones found in good natured® (*Good Natured Products*, 2020) and Vegware$^{\text{TM}}$ (Vegware, 2020), LivBar®, which, produces energy bars with a compostable wrapper (LivBar, 2020). It's also possible to find cluttery made from starch and other biodegradable materials in GreenGate® (GreenGate, 2020).

1.2 Hemicellulose and its film-forming ability

1.2.1 Hemicellulose and Xylan

Hemicellulose is an important component of plant cell walls, responsible for the rigidity structure of cell walls. (Fundador *et al.*, 2012) It's also one of the most abundant renewable resources available, along with cellulose and starch. To extract this component from plant tissues, different treatments are employed, such as using an alkaline solution, dimethyl sulfoxide, methanol/water, steam, or microwave treatment. The type of treatment significantly influences the composition of the final extract. (Hansen and Plackett, 2008; Belmokaddem *et al.*, 2011)

In comparison with starch and cellulose, hemicellulose potential uses haven't been properly explored. It's commonly discarded as waste material or used to produce ethanol, acetone, butanol, and xylitol. (Fundador *et al.*, 2012) There's been, however, an increase of research related to this natural resource. (Shao *et al.*, 2019) Due to its gel and film-forming properties, biocompatibility and biodegradability, it's been investigated some applications like drug delivery, cellular therapy, packaging and coatings. (Hansen and Plackett, 2008)

In its structure it can include different polysaccharides: xylan, glucuronoxylan, arabinoxylan, mannan, glucomannan and galactoglucomannan. Hemicellulose presents an heterogenous composition of diverse sugar units that are classified depending on the type of linkage and unit: xylans (β-1,4 linked D-xylose units), mannans (β-1,4 linked D-mannose units), arabinans (α-1,5 linked L-arabinose units) and galactans (β-1,3 linked D-galactose units). This represents the main (sugar) backbone of hemicellulose structure, which is also usually substituted with side chains. (Belgacem and Gandini, 2008)

Xylan is one of the predominant constituents of hemicellulose, having a linear backbone of β-1,4 linked D-xylopyranose units, that can be substituted with other residues such as acetyl, arabinosyl and glucuronosyl. (Belgacem and Gandini, 2008) It can be commonly found and extracted from different agricultural products such as wheat straw, corn stalks and cob, sugar cane and soft or hardwood obtained from forest and pulping waste. (Kayserilioğlu *et al.*, 2003)

1.2.2 Natural based films

Hemicellulose films are biodegradable and biocompatible. Besides, they show low fat and low oxygen permeability when dehydrated. They are, however, sensitive to moisture and completely soluble in water. (Zoldners and Kiseleva, 2013; Shao *et al.*, 2019)

As a consequence, the increase of their water-resistant properties is highly necessary. Some techniques to achieve this comprises the removal of the hydroxylic groups (through various chemical reactions) or the use of cross-linking reactions. (Zoldners and Kiseleva, 2013; Shao *et al.*, 2019) Cross-linking agents include bi or polyfunctional compounds such as aldehyde based reagents or polycarboxylic acids. (Zoldners and Kiseleva, 2013)

Glutaraldehyde is a dialdehyde that can be used as a cross-linker, however this compound shows great toxicity likewise other aldehydes. (Zoldners and Kiseleva, 2013; Xiang *et al.*, 2016) A safer option is the use of polycarboxylic acids such as citric acid, oxalic acid, maleic acid, succinic acid, and malonic acid (Figure 1.8). (Zoldners and Kiseleva, 2013) Citric acid (PubChem, 2020a) is used as a flavoring agent, succinic acid (PubChem, 2020e) may be used as nutritional supplementation and is a food additive, malonic acid (PubChem, 2020c) is also a food addictive, maleic (PubChem, 2020b) and oxalic (PubChem, 2020d) acid are only used indirect food additives and may contain some toxicity.

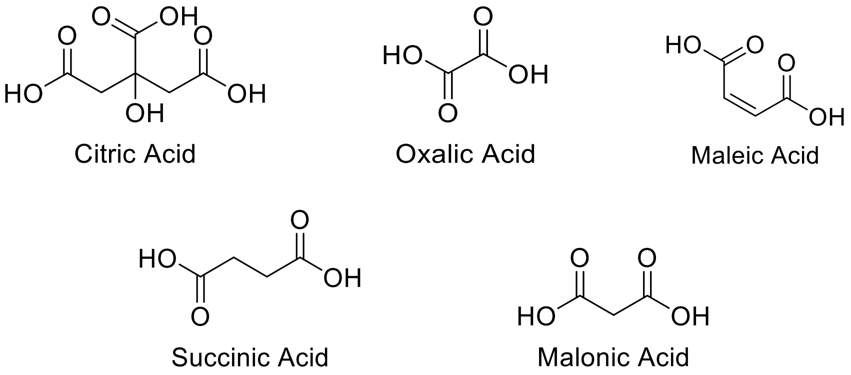

Citric Acid
Oxalic Acid
Maleic Acid
Succinic Acid
Malonic Acid

Figure 1.8: Chemical structure of different polycarboxylic acids.

Another way to improve the mechanical properties of natural-based films is by adding a plasticizer (usually a polyol, like glycerol or sorbitol, Figure 1.9). The plasticizer can allocate itself between the polysaccharide chains reducing their intermolecular interactions and changing the three-dimensional structure. (Vieira *et al.*, 2011), reducing films brittleness and increasing their flexibility and deformability. (Mikkonen *et al.*, 2009; Vieira *et al.*, 2011)

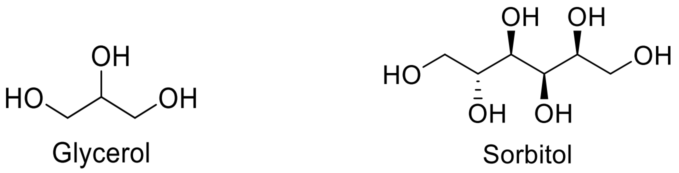

Glycerol
Sorbitol

Figure 1.9: Chemical structure of different polyols.

1.3 Arabinoxylan as resource

1.3.1 Arabinoxylan

Arabinoxylan (Ax) is comprised by a linear xylan backbone linked by β-1,4 bonds and usually a single arabinose substituent in O2 and/or O3 (it's also possible not to have any substituent as side chain). The arabinose residues are also often esterified with ferulic acid (Figure 1.10). (Belgacem and Gandini, 2008; Anderson and Simsek, 2019b)

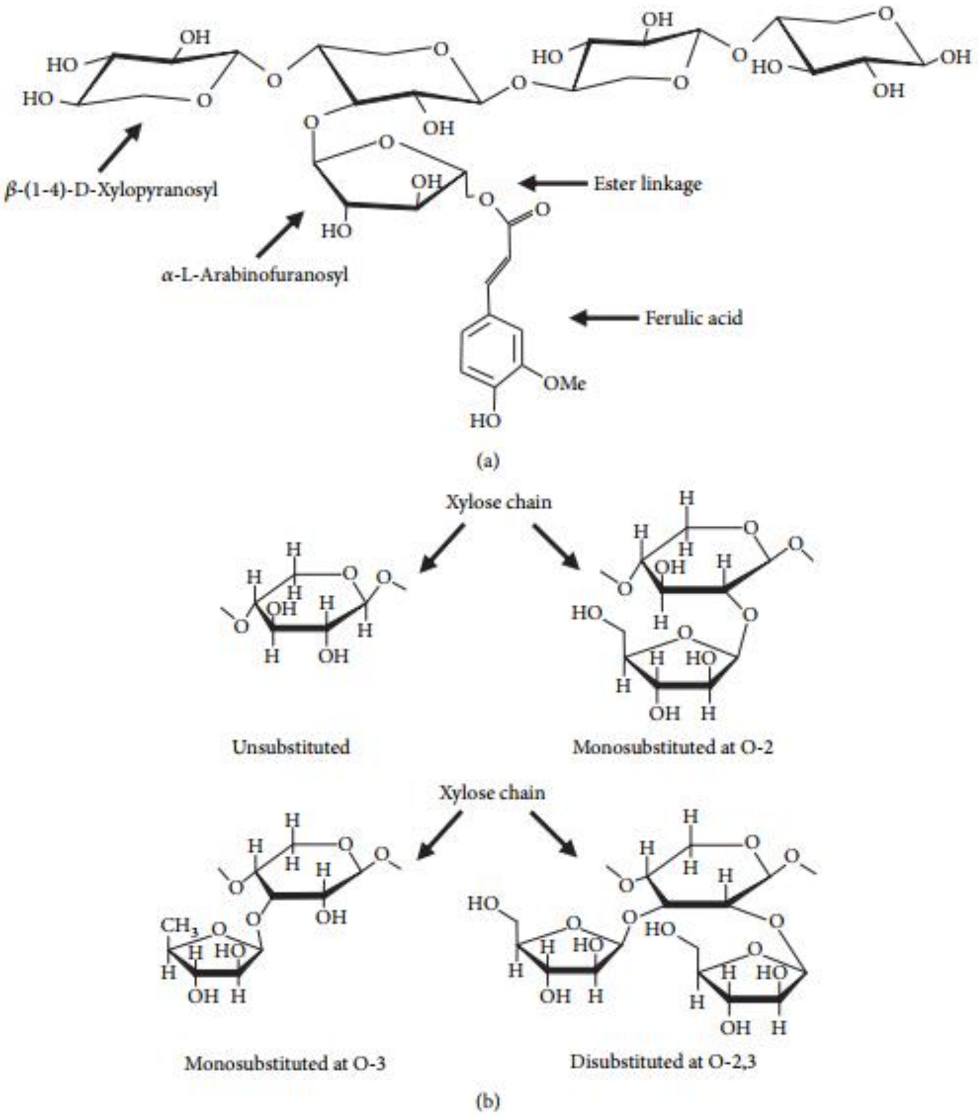
β-(1-4)-D-Xylopyranosyl
α-L-Arabinofuranosyl
Ester linkage
Ferulic acid
(a)
Xylose chain
Unsubstituted
Monosubstituted at O-2
Xylose chain
Monosubstituted at O-3
Disubstituted at O-2,3
(b)

Figure 1.10: (a) Representation of the chemical structure of arabinoxylan and its linkages (b) Possible arabinose substituents present in the arabinoxylan chain. (source: (Mendez-Encinas *et al.*, 2018))

The biosynthesis of arabinoxylan is a polymerization process that includes chain initiation, elongation, and termination. During the polymerization process arabinose and feruloyl groups are added to the main backbone chain. After the deposition of the feruloylated arabinoxylans in the cell walls, cross-linking can occur between them. This modification can alter their physicochemical properties (solubility and interaction with other polysaccharides) allowing the plant to manage the permeability of cell walls, tissue cohesion and expansion of the cell. (Zhurlova, 2017)

Arabinoxylan can be found in major cereal grains, like wheat, oats, rice, corn, barley, millet, and rye. (Belgacem and Gandini, 2008; Zhurlova, 2017; Anderson and Simsek, 2019b) It's also found in other plants such as psyllium, pangola grass, bamboo shoots and rye grass. The percentage of arabinoxylan in each cereal is different since it's highly dependent on genetic and environmental characteristics. (Zhurlova, 2017)

The extraction of arabinoxylan is commonly achieved by aqueous or alkaline extraction. Since arabinoxylan are cross-linked these interactions are not easily broken in a simple aqueous environment, therefore an alkaline environment helps break down covalent and non-covalent bonds. (Zhurlova, 2017)

Thus, arabinoxylans extracted with only water are considered water soluble. The arabinoxylans that are cross-linked and require extra steps (alkaline solution) to be extracted are considered water insoluble. (Zhurlova, 2017)

Arabinoxylan (from corn bran or corn fiber) is reported to have a molecular weight of 253/362kDa (Kale *et al.*, 2018) or 264.2±9.72kDa (when extracted at 25°C)(Yan *et al.*, 2019).

1.3.2 Corn bran and corn fiber

Corn (Figure 1.11) can be processed by dry-milling or wet-milling. The dry-milling technique is the traditional way to separate corn into its endosperm, germ, and bran. The endosperm is recovered to be used as corn grits, meals and flours, the germ may be used for oil and the corn bran is a low-value product that is currently used as animal feed. In wet-milling, the corn is first soaked in water and sulfur dioxide, then it's separated into starch, gluten, fiber and germ. Starch (obtained from the endosperm) and oil (obtained from the germ) are profitable products. Other products from this processing are corn fiber, corn gluten and other solids from the soaking process, that are usually combined and commercialized as corn gluten feed.(Rose, Inglett and Liu, 2010)

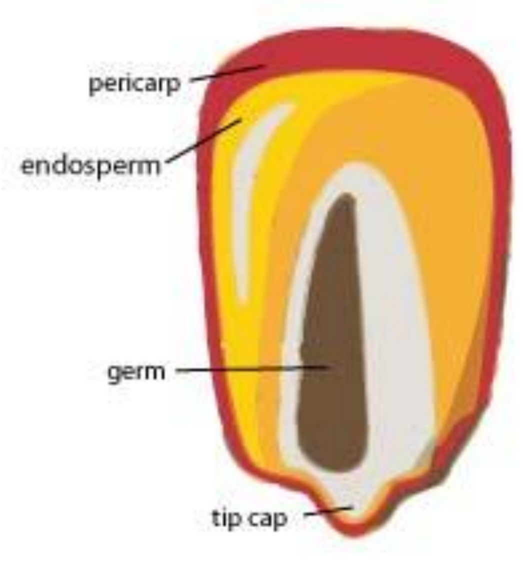

Figure 1.11: The various components that form a corn kernel. (source: (Association, 2020))

The main component of corn fiber and corn bran is the pericarp, plus the first one contains cell wall material from the endosperm. These co-products are usually considered low-value products, since they're used as animal feed, therefore new applications are constantly being explored. (Rose, Inglett and Liu, 2010)

The major constituents in both corn bran and fiber are hemicellulose, cellulose, and a small proportion of lignin. Also, the hemicellulose fraction is mainly comprised by arabinoxylan (Table 1.1). (Rose, Inglett and Liu, 2010)

Table 1.1: Composition of corn barn compared to corn fiber in g/kg. (source: (Rose, Inglett and Liu, 2010))

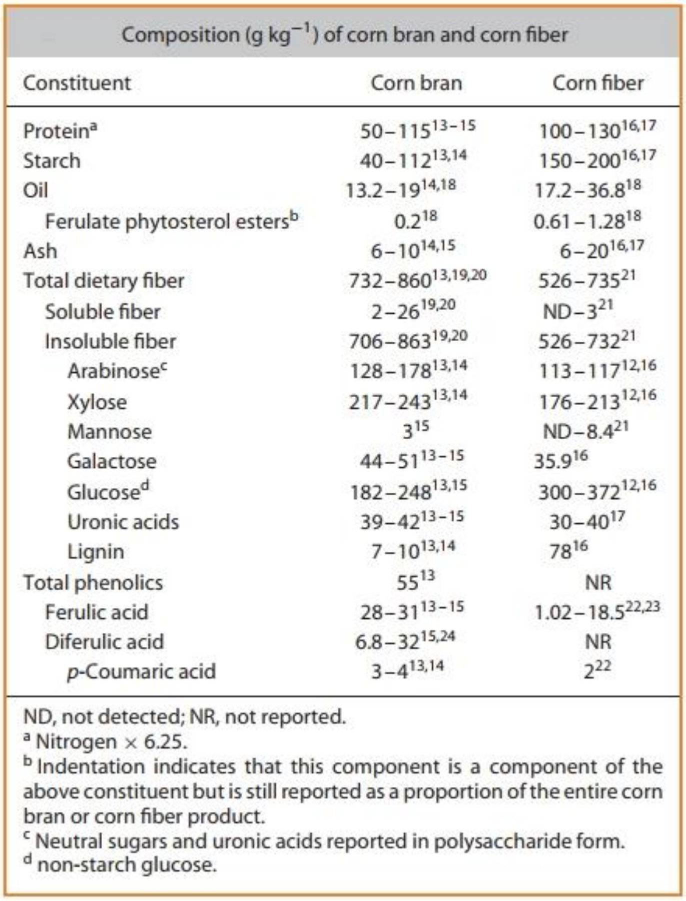

Composition ($g\ kg^{-1}$) of corn bran and corn fiber

Constituent	Corn bran	Corn fiber
Protein[a]	50–115[13–15]	100–130[16,17]
Starch	40–112[13,14]	150–200[16,17]
Oil	13.2–19[14,18]	17.2–36.8[18]
Ferulate phytosterol esters[b]	0.2[18]	0.61–1.28[18]
Ash	6–10[14,15]	6–20[16,17]
Total dietary fiber	732–860[13,19,20]	526–735[21]
Soluble fiber	2–26[19,20]	ND–3[21]
Insoluble fiber	706–863[19,20]	526–732[21]
Arabinose[c]	128–178[13,14]	113–117[12,16]
Xylose	217–243[13,14]	176–213[12,16]
Mannose	3[15]	ND–8.4[21]
Galactose	44–51[13–15]	35.9[16]
Glucose[d]	182–248[13,15]	300–372[12,16]
Uronic acids	39–42[13–15]	30–40[17]
Lignin	7–10[13,14]	78[16]
Total phenolics	55[13]	NR
Ferulic acid	28–31[13–15]	1.02–18.5[22,23]
Diferulic acid	6.8–32[15,24]	NR
p-Coumaric acid	3–4[13,14]	2[22]

ND, not detected; NR, not reported.
[a] Nitrogen × 6.25.
[b] Indentation indicates that this component is a component of the above constituent but is still reported as a proportion of the entire corn bran or corn fiber product.
[c] Neutral sugars and uronic acids reported in polysaccharide form.
[d] non-starch glucose.

As seen in Table 1.1, both corn bran and corn fiber contain a significant amount of phenolic acids in their composition. Besides ferulic and ρ-coumaric acid, it may also be possible to find other phenolic compounds such as: protocatechuic, vanillic, sinapic, syringic, ρ-hydroxybenxoic, caffeic, isoferulic acids, cyanidin-3-O-glucoside, kaempferol, quercetin. These compounds are most likely found and concentrated in the pericarp and germ, respectively and can be related to the color of the grain. (Preedy and Watson, 2019)

Besides the presence of these compounds, it’s also reported that the typical yellow color from corn is due to the presence of carotenoids, more specifically xanthophylls (carotenoids with oxygen in their structure), like zeaxanthin and lutein. β-carotene is also another carotenoid that is reported to be responsible for the yellow color. (Sessa *et al.*, 2003; Preedy and Watson, 2019)

In the outer bran layers (pericarp) and the germ of corn it’s possible to find in significant quantities carotenoids, anthocyanins and phenolic compounds. Carotenoids can be very diverse, the most abundant ones found in corn are lutein and zeaxanthin, it's also possible for α-cryptoxanthin, β-cryptoxanthin, α-carotene and β-carotene to be part of the composition in a smaller quantity. (Preedy and Watson, 2019)

1.3.3 Arabinoxylan applications

Arabinoxylan is a major component in the dietary fiber fraction of cereal grains intake of humans. (Broekaert *et al.*, 2011) It is known that consuming arabinoxylan (2-10g/day) reduces cholesterol and has an impact in reducing the concentration of blood glucose, fructosamine and insulin. (Zhurlova, 2017) Arabinoxylan also potentially prevents colon cancer, overgrowth of pathogenic bacteria in the intestine and cardiovascular disease. (Zhurlova, 2017; Anderson and Simsek, 2018) Ferulic acid is an antioxidant and anti-inflammatory and since it's bound to arabinoxylan it can bring additional benefits. In this way, introducing arabinoxylan in various food products can bring benefits to our health. (Zhurlova, 2017)

The addition of 0.5% of arabinoxylan to bread increased its volume and had a positive effect on the texture (water soluble arabinoxylan seemed to improve the viscosity of the aqueous phase of the dough). However, at 1% of arabinoxylan the addition had a negative impact in gluten strength (water insoluble arabinoxylan seems to alter gluten structural network). (Zhurlova, 2017)

Water soluble arabinoxylan can be used as a cryo-stabilizing agent to prevent the formation of ice crystals when the dough is frozen or refrigerated and also prevents starch crystallization associated with the staling of baked products. (Anderson and Simsek, 2018)

In summary, some approaches have been made in order to include this co-product in food like bread, cake and muffins, however its addition sometimes brought undesired changes into the final product, therefore more research must be done in order to achieve the desired quality of the product. (Rose, Inglett and Liu, 2010)

Besides food applications, arabinoxylan was also found to be useful as films and coatings. Arabinoxylan films from oat spelt were previously prepared with glycerol, sorbitol and xylitol as plasticizer. Xylitol showed migration and/or crystallization on the film surface, therefore it couldn't be used as plasticizer. The addition of NaAc or NaCl (even in small quantities) had a negative impact on tensile strength of the films produced. (Mikkonen *et al.*, 2009). In addition, emulsified arabinoxylan films were prepared with a blend of lipids (palmitic acid, oleic acid, triolein or hydrogenated palm oil) and glycerol as plasticizer. (Péroval *et al.*, 2002)

Arabinoxylan extracted from distiller's grains and sugarcane bagasse was previously cross-linked with glutaraldehyde to be used a paper coating. (Li *et al.*, 2020)

Hydrogels (a polymeric network that are able to retain large amounts of water and not dissolve (Ahmed, 2015)) produced from arabinoxylan can be easily achieved by using agents that can create free radicals. These gels can be used in drug delivery systems. (Anderson and Simsek, 2018)

However, since arabinoxylan is not available in its pure form in nature, it's necessary to first extract it from a source with a significant amount. Then, to obtain an extract rich in arabinoxylan, a purification step is required.

1.3.4 Extraction and Purification of Arabinoxylan

Arabinoxylan was previously extracted with water, alkaline or acid solution or an enzymatic treatment. (Zhang, Smith and Li, 2014)

Extraction of arabinoxylan with water is a quite common method of extraction, however it only yields water soluble fractions of arabinoxylan, meaning that it's only useful when only that fraction is desired. (Zhang, Smith and Li, 2014)

Enzymatic treatment of arabinoxylan is another possible method of extraction, however it was found that the yields of this process were lower when compared with alkaline or acid treatments. For this type of treatment, it's necessary to choose an adequate enzyme, consider the crystalline structure of the raw material as well as the presence of possible enzyme inhibitors. (Zhang, Smith and Li, 2014)

Arabinoxylan was previously extracted with an acid solution, however it was found that this extraction lead to an extensive acid catalyzed hydrolysis, meaning that part of the arabinoxylan was degraded to low molecular fractions which can easily be lost in future purification steps. (Zhang, Smith and Li, 2014)

Alkaline extraction is a highly efficient method and has been employed as early as 1900, to treat various cereals bran, including arabinoxylan, with NaOH being one of the most common reagents. This extraction is a simple method, in which the hydrogen, covalent and ester bonds are disrupted allowing the release of components from the cell wall to the solution. (Zhang, Smith and Li, 2014)

After extraction, the raw extract needs to be further purified or enriched. Ethanol fractionation was applied to separate arabinoxylan into different fractions according to their arabinose/xylan ratio and degree of substitution. (Zhang, Smith and Li, 2014; Anderson and Simsek, 2019a). Another purification method is dialysis, which it was used to remove small contaminants from arabinoxylan from corn bran. (Anderson and Simsek, 2019a)

Purification methods with membranes are easily operated processes that allow both the concentration of the polysaccharides, like arabinoxylan, and the removal of small contaminants. (Serra *et al.*, 2020) This method will be discussed more in depth in next chapter (1.4) as the one chosen to be employed in this work.

1.4 Separation processes

1.4.1 Types of separation

It's often desirable to separate different components present in a complex mixture. Different separation processes can be applied depending on the components present and, especially, their physical and chemical properties. Below, Table 1.2 shows a small list of some separation processes relative to the physical/chemical properties of the components (Mulder, 1997)

Table 1.2: Different separation processes according to physical/chemical properties of the components. (adapted from: (Mulder, 1997))

Physical/chemical property	Separation process
Size	Filtration, microfiltration, ultrafiltration, dialysis, gas separation, gel permeation chromatography
Vapor pressure	Distillation, membrane distillation
Freezing point	Crystallization
Affinity	Extraction, adsorption, reverse osmosis, gas separation, pervaporation, affinity chromatography
Charge	Ion exchange, electrodialysis, electrophoresis, diffusion dialysis
Density	Centrifugation
Chemical nature	Complexation, carrier mediated transport

Besides the physical/chemical properties of the components, it's also useful to consider the size of the components that we're trying to separate. Figure 1.12 below presents some separation processes according to the primary factor affecting the separation as well as the range the process allows a good quality separation.

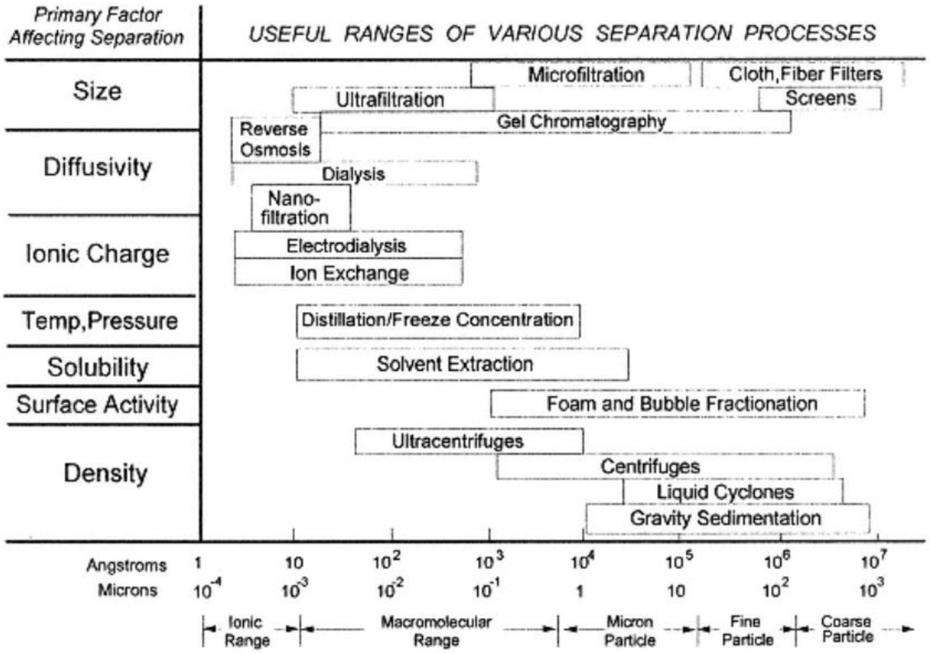
Primary Factor Affecting Separation
USEFUL RANGES OF VARIOUS SEPARATION PROCESSES
Size
Diffusivity
Ionic Charge
Temp,Pressure
Solubility
Surface Activity
Density
Microfiltration
Cloth,Fiber Filters
Ultrafiltration
Screens
Reverse Osmosis
Gel Chromatography
Dialysis
Nano-filtration
Electrodialysis
Ion Exchange
Distillation/Freeze Concentration
Solvent Extraction
Foam and Bubble Fractionation
Ultracentrifuges
Centrifuges
Liquid Cyclones
Gravity Sedimentation
Angstroms
Microns
Ionic Range
Macromolecular Range
Micron Particle
Fine Particle
Coarse Particle

Figure 1.12: Various possible separation processes according to different factors and their respective range of separation. (source: (Cheryan, 1998))

Therefore, besides the characteristics of the components present in the mixture and other factors, it’s also important to consider whether the separation process is technically feasible (if the process is able to achieve the desired separation with a good product enrichment/purification) and economically when choosing which method(s) to be applied. (Mulder, 1997)

1.4.2 Membranes

Various membrane technologies are vastly used in a broad range of applications, they may allow the permeation of specific chemical species, making it possible to tune which species permeate through the membrane materials. A membrane can then be described as a “thin interface that regulates the permeation of chemical species in contact with it”, it’s also defined as a “selective barrier”. (Cheryan, 1998; Mohanty and Purkait, 2011)

Membranes can be classified according to various characteristics: (Cheryan, 1998; Mohanty and Purkait, 2011)

-Physical state (liquid or solid)
-Nature (natural or synthetic)
-Structure (porous/heterogeneous or nonporous/homogeneous)
-Symmetry (isotropic or anisotropic)
-Application (gas-gas, gas-liquid or liquid-liquid separation)
-Mechanism (adsorption, diffusion, ion-exchange, osmose or nonselective)

1.4.3 Membrane processes

Membrane processes have a major role in laboratory and industrial processes (for example, in the food and petrochemical industry). They can be used as replacement of traditional methods (especially those that include high temperature or to avoid adding preservatives/additives) or as a new technique. (Takht Ravanchi, Kaghazchi and Kargari, 2009; Dhineshkumar and Ramasamy, 2017)

Membrane processes are considered a green technology since they may be efficient methods in terms of energy spent and may not require the utilization of toxic chemicals. Another great usage of this technique is that it allows the recovery of valuable products from wastewater, by-products and effluents. (Dhineshkumar and Ramasamy, 2017)

In pressure-driven membrane processes, the basic principle is that a feed stream is pumped through a module (where the membrane is placed), due to a certain driving force created between the feed and permeate streams (which in this case is the gradient of total pressure).

One being the retentate/concentrate (molecules that are not able to permeate through the pores of the membranes, for example, macromolecules) and the other is the permeate (solvent and smaller components that are able to permeate through the pores of the membranes). (Figure 1.13) One of these streams is the product and will be enriched with one or more components. (Mulder, 1997; Cheryan, 1998)

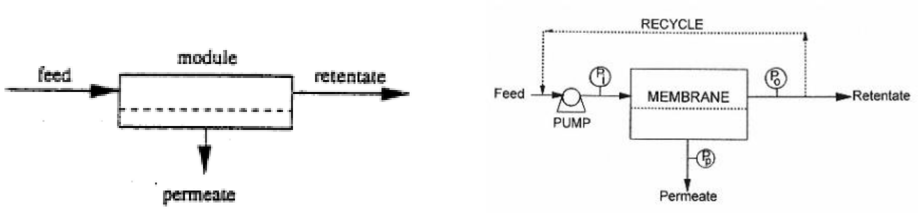

Figure 1.13: Basic principle of a separation process (left), example of a setting of a membrane process (right). (source: (Mulder, 1997; Cheryan, 1998))

Depending on its objective, the process can be classified as:

-Concentration (the component desired is in low concentration and the solvent is to be removed)
-Purification (remove undesired components/impurities)
-Fractionation (separation of two or more desired components from a complex mixture)
-Reaction mediation (removal of product is combined with a (bio)chemical reaction, consequently increasing the reaction rate)

Some pressure-driven membrane separation processes include reverse osmosis, nanofiltration, ultrafiltration, microfiltration. (Mohanty and Purkait, 2011; Dhineshkumar and Ramasamy, 2017)

Reverse osmosis is a process commonly used in the purification of saline water. The feed is concentrated with solute and is pressurized and forced through a semi-permeable membrane, the permeate may consist in the solute free solvent. (Qin *et al.*, 2019) Membranes for reverse osmosis should have very small pores, in the range of 3-5Å in diameter, where ideally only water (or the solvent) should permeate through, these membranes are also often considered to be nonporous since the membrane pores are very small. (Mohanty and Purkait, 2011)

Ultrafiltration, microfiltration and nanofiltration processes are different from reverse osmosis, as the first have clear pores, and consequently different components permeate through the membrane. (Cheryan, 1998; Mohanty and Purkait, 2011) Below, it’s presented an example of which components are usually able to permeate through each membrane and which ones are retained. (Figure 1.14)

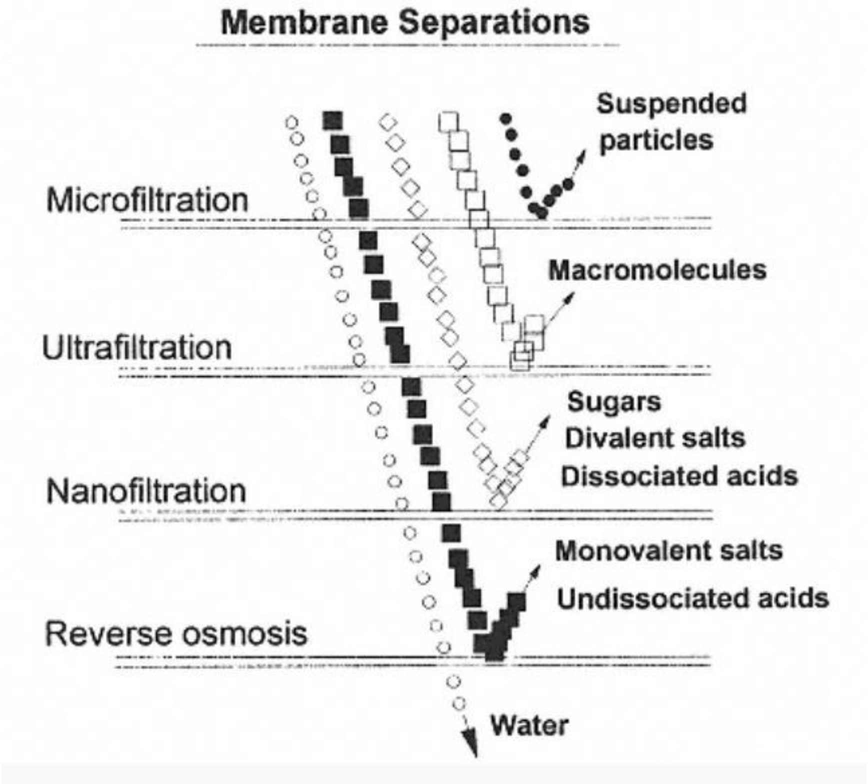
Membrane Separations
Suspended particles
Microfiltration
Macromolecules
Ultrafiltration
Sugars
Divalent salts
Dissociated acids
Nanofiltration
Monovalent salts
Undissociated acids
Reverse osmosis
Water

Figure 1.14:Components that each membrane separation is usually able to split up. (source: (Cheryan, 1998))

Moreover, these membrane processes are vastly employed in very diverse fields and are known to be used to separate solutes like pollen, albumin and glucose. (Figure 1.15) Some other molecules such as natural polymers, including proteins, starch, gums and colloidal dispersed compounds like clays, paints, pigments, latex particles can be separated by ultrafiltration. (Cheryan, 1998)

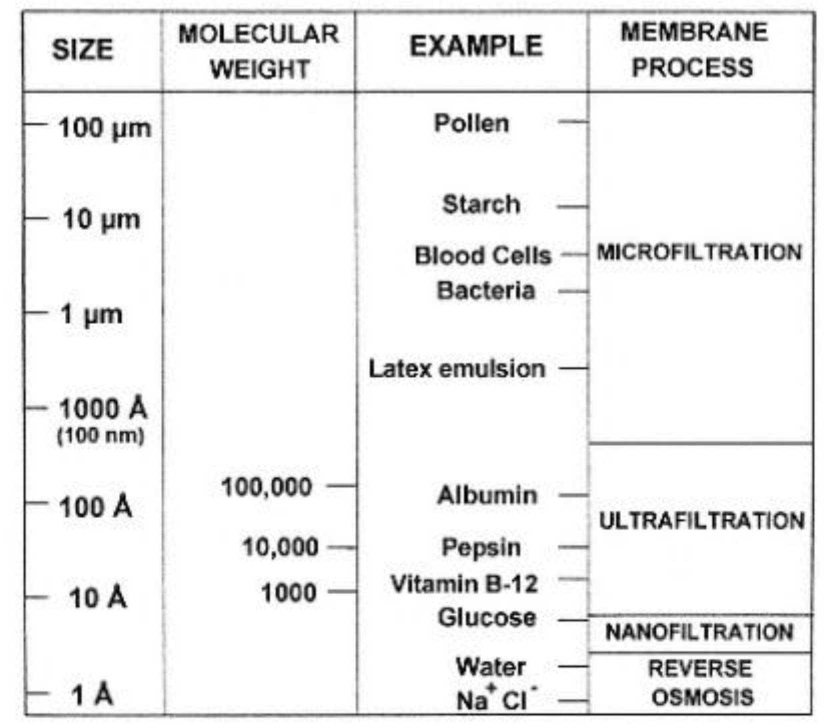
SIZE
MOLECULAR WEIGHT
EXAMPLE
MEMBRANE PROCESS
100 µm
10 µm
1 µm
1000 Å (100 nm)
100 Å
10 Å
1 Å
100,000
10,000
1000
Pollen
Starch
Blood Cells
Bacteria
Latex emulsion
Albumin
Pepsin
Vitamin B-12
Glucose
Water
Na⁺ Cl⁻
MICROFILTRATION
ULTRAFILTRATION
NANOFILTRATION
REVERSE OSMOSIS

Figure 1.15: Membrane processes according to the size of the component. (source: (Cheryan, 1998))

Microfiltration membranes have usually pores with 10000Å of diameter, while ultrafiltration pores are 100x smaller and reverse osmosis pores are 1000x smaller (Figure 1.16). (Mohanty and Purkait, 2011)

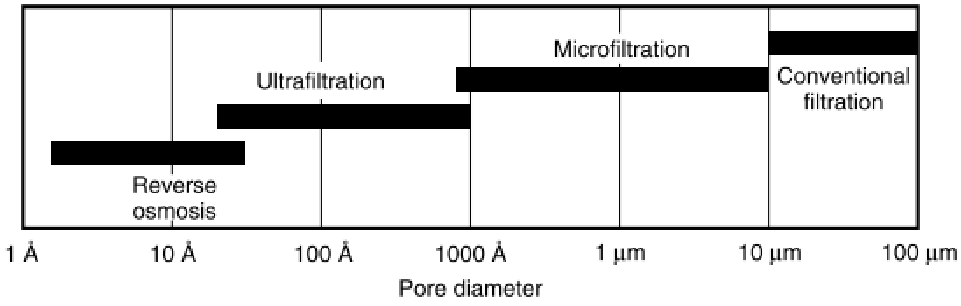

Figure 1.16: Pore diameter of each membrane process. (source: (Mohanty and Purkait, 2011))

1.4.4 Membrane transport/Mechanism of permeation

Membrane transportation is based in two different models: solution-diffusion and pore-flow. (Mohanty and Purkait, 2011)

In solution-diffusion, the permeants are able to dissolve into the membrane and diffuse through it. The different solubilities and diffusion rates allow a separation of the various permeants. In this model the pores are essentially small spaces that appear between the polymer chains during the thermal motion. This model applies to membranes with a dense behavior, used in reverse osmosis (Mohanty and Purkait, 2011)

In pore-flow the permeants are forced through tiny pores in the membrane while in a pressure driven flow. The separation occurs since only some permeants are able to go through the membrane pores. Contrary to the model mentioned above, in this process the membrane pores are fixed, not changing its volume and position during the separation process (Figure 1.17). This model applies to micro-/ultra-nano-filtration processes. (Mohanty and Purkait, 2011)

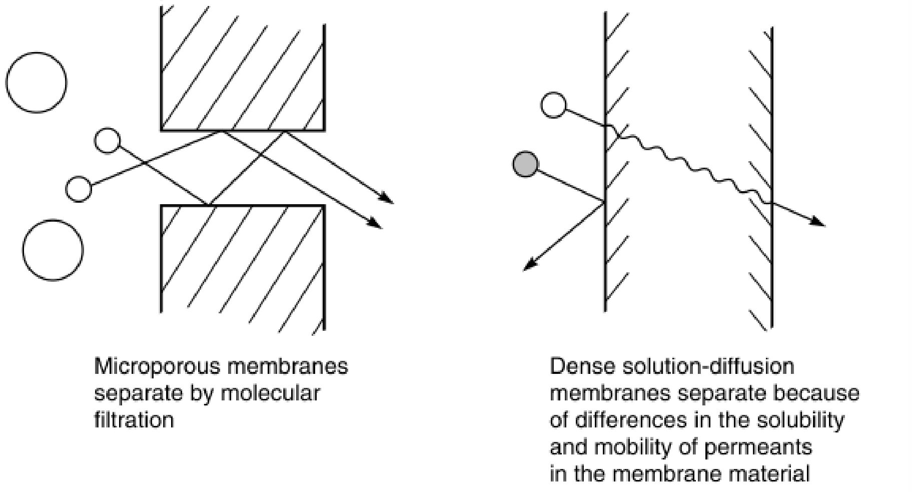
Microporous membranes separate by molecular filtration
Dense solution-diffusion membranes separate because of differences in the solubility and mobility of permeants in the membrane material

Figure 1.17: Different mechanisms of permeation: pore-flow (left) and solution-diffusion (right). (source: (Mohanty and Purkait, 2011))

Both ultrafiltration and microfiltration processes operate following the pore-flow model. Membranes used for reverse osmosis and pervaporation processes don't have definite pores, following the solution-diffusion model. Some processes don't follow completely one model, which is the case with nanofiltration. (Figure 1.18) (Cheryan, 1998; Mohanty and Purkait, 2011)

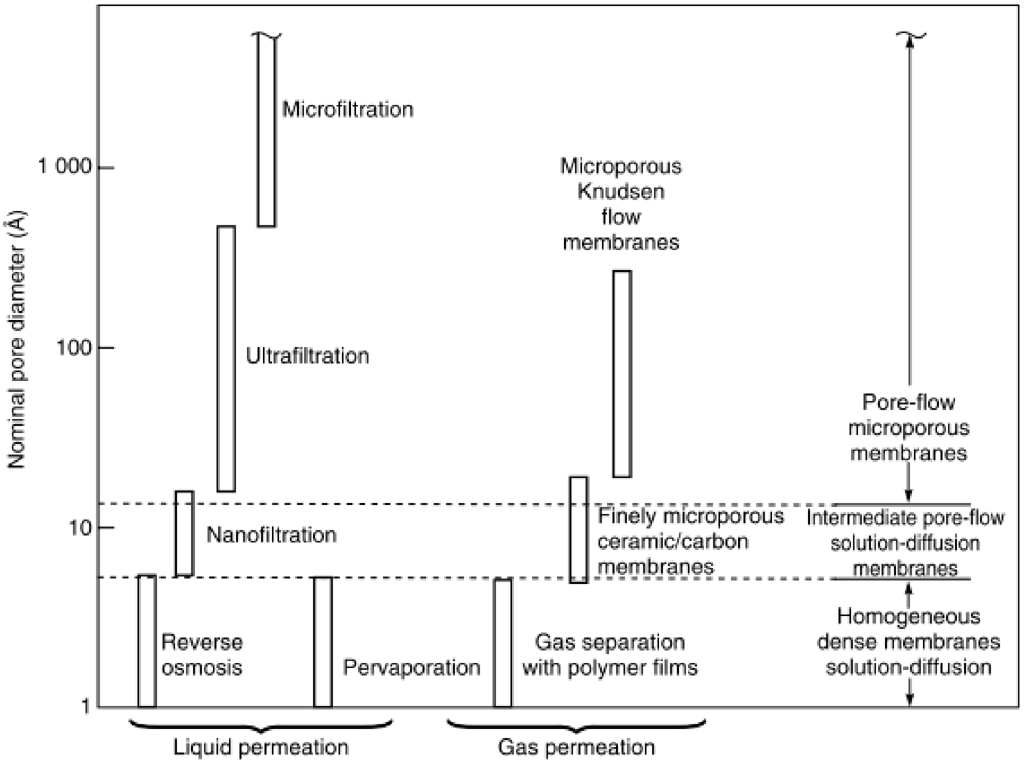

Figure 1.18: Different membrane processes and their respective mechanism of permeation. (source: (Mohanty and Purkait, 2011))

1.4.5 Parameters of membrane processes

To understand the membrane process, it’s important to know and define some parameters.

Rejection (R_i) is a parameter that allows us to analyze the performance of the process, it represents the capacity to retain molecules of a particular size. Rejection is calculated by the following Equation 1.1: (Scott, 1998)

$$R_i = 1 - \frac{C_{perm}}{C_{feed}} \qquad \text{(Equation 1.1)}$$

Where C_{perm} (g/L) is the concentration in the permeate and C_{feed} (g/L) is the concentration in the feed. The values of rejection depend on various factors related to the operation and vary between 0 and 1. When rejection is close to 1, molecules are retained and don’t permeate through the membrane, on the other hand when rejection is close to 0 most of the molecules pass through the membrane and are permeated.

Permeate volumetric flux (J_v, $L{\cdot}h^{-1}{\cdot}m^{-2}$) indicates the quantity (in volume) of liquid that passes through the membrane per unit of time and per membrane area. (Scott, 1998) It’s expressed by the following Equation 1.2:

$$J_v = \frac{Q}{A_m} \qquad \text{(Equation 1.2)}$$

Where Q is the volumetric flowrate (L/h) and A_m is the area of the membrane (m^2).

Permeability (L_p, $L{\cdot}h^{-1}{\cdot}m^{-2}{\cdot}bar^{-1}$) relates the variation of the permeate flux with the pressure.

$$L_p = \frac{J_v}{P} \qquad \text{(Equation 1.3)}$$

Where J_v is the flux ($L{\cdot}h^{-1}{\cdot}m^{-2}$) and P (bar) is the pressure.

The percentage of solutes removed from the initial solution can be calculated directly by the following Equation 1.4:

$$\%rem = 1 - \frac{C_{fi}}{C_{f0}} \times 100 \qquad \text{(Equation 1.4)}$$

Where C_{fi} (g/L) is the concentration of solutes in the feed at the instant i and C_{f0} (g/L) is the concentration of salts in the feed at the beginning.

The Reynolds number (Re) is a very important parameter in fluid dynamics that indicates how the liquid flows inside the membrane (in laminar or turbulent regimes, usually for the laminar regime Re<2000 and for the turbulent regime Re>4000). (Holman, 2010)

$$Re = \frac{\rho v D}{\mu} \qquad \text{(Equation 1.5)}$$

Where, ρ (kg/m^3) is the density of the fluid, v is the velocity of the fluid (m/s), D (m) is the diameter of the tube where the fluid is passing through and μ is the dynamic viscosity of the fluid (Pa.s).

1.4.6 Types of membrane configuration

There are essentially 4 types of designs for membranes: (Cheryan, 1998)

-Tubular (inner diameter >4mm)
-Hollow fibers
-Plate unit

-Spiral-wound module

In tubular modules polymeric membranes are placed inside of tubes (serving as supports), different internal diameters are possible as well as different materials of which the tubes are made of. Various tubes can also be enclosed together, to form the module. It can be applied for reverse osmosis, ultrafiltration and microfiltration processes. (Cheryan, 1998)

Hollow fibers membranes are similar to tubular modules, however the membrane doesn't need a supporting tube, since the membrane has a tubular form itself. The only support needed for this module is an outer shell where all the tubes are assembled. Each tube or fiber has an internal diameter of <1mm. It can be used for ultrafiltration and microfiltration processes and reverse osmosis with some slight changes. (Cheryan, 1998)

Plate units are comprised of flat plate, followed by a channel for the permeate and finally a flat sheet of membrane, this configuration can be mirrored to form the whole plate. Various of these units can be put together to form a bigger module. (Cheryan, 1998)

In spiral-wound modules, two flat sheet membranes are separated by a spacer and glued to a pierced tube in the middle (this is where the permeate will flow into), on the outside side there's another spacer where the feed will flow. This whole unit is rolled around the tube in the middle. (Cheryan, 1998)

1.4.7 Operation modes

Membrane processes like ultrafiltration can be operated into different modes. In direct ultrafiltration (also known as concentration) no alteration in the system is made, therefore the permeate is continuously collected and the feed is getting increasingly concentrated. Consequently, the viscosity in the feed is also increasing, reducing the flux and making it necessary to increase the pumping power. (Cheryan, 1998)

A more efficient way to generally purify certain (big) solutes in a solution by ultrafiltration is using diafiltration mode, in which deionized water is added to the retentate and those solutes are retained on the membrane. (Cheryan, 1998) Each time the volume of water added is equivalent to the volume of the (original) feed, it is counted a diavolume.

Diafiltration can also be run in discontinuous or continuous mode.

In discontinuous mode, the feed is purified by direct ultrafiltration, then water is added, and the feed is again purified, these steps can be repeated as many times as necessary. In continuous mode water is added at a similar rate as the permeate is collected and the volume in the feed remains constant. This mode avoids the concentration of the feed, while still allowing its purification. (Cheryan, 1998) In this case, it's important that the volumetric flowrate of water added to be identical to the flowrate of the permeate.

These processes are usually run in cross flow mode, instead of the conventional dead-end mode. In the dead-end mode, the feed runs perpendicular to the membrane, with time the particles that are retained will accumulate in the membrane surface decreasing the permeation rate. In cross flow mode, however, the flow runs parallel to the membrane avoiding the rapid accumulation of retained particles in the membrane. (Scott, 1998)

1.5 Thesis outline and objectives

Corn fiber is a by-product of the starch industry and one of its main applications is animal feed, however corn fiber contains ferulic acid a known antioxidant, and arabinoxylan with film-forming properties. The main goals of this thesis are to achieve a good quality purified extract that can later be used to obtain films. These films are later formulated with plasticizers, cross-linkers and other components to improve their properties.

This thesis was organized in three parts, the first is focused on the extraction and purification (with membrane filtration) of arabinoxylan from corn fiber, the second in the optimization of this purified extract to be later formulated into films, lastly the third part was dedicated to study mechanical and antioxidant properties, solubility in water and color of the obtained films.

2. Materials and Methods

2.1 Materials

Corn fiber from Copam Companhia Portuguesa De Amidos, S.A. was used in this work. For extraction NaOH (pellets, eka) was used. In the purification process a hollow-fiber membrane (UFP-100-C-5A, from GE Healthcare, USA) was chosen. The membrane is made of polysulfone, with a flow path of 30 cm and area of 0.2m^2, the molecular weight cut-off (MWCO) is 100kDa. For membrane cleaning alkaline Ultrasil 110 (Ecolab, Canada), acid Ultrasil 75 (Ecolab, Canada) and ethanol (96%, Labchem) were utilized.

For the decolorization process it was used activated charcoal or hydrogen peroxide (130vol., José Manuel Gomes dos Santos LDA). For the formulation of films glycerol (≥99%, Sigma-Aldrich), malonic acid (99%, Sigma-Aldrich), citric acid (99.5%, PanReac), succinic acid (≥99.5%, Sigma-Aldrich), sodium hypophosphite monohydrate (≥99%, Sigma-Aldrich) and NaOH (pellets, eka). For the determination of antioxidant activity acetate buffer (99.5%, Riedel-de Haën), TPTZ (≥99%, Sigma-Aldrich), HCl (≥37%, Honeywell), ferric chloride (98%, Panreac).

2.2 Extraction of Arabinoxylan

Arabinoxylan was extracted with an alkaline solution of NaOH 0.25M for 7h at 30°C, with stirring. It was then centrifugated (Avanti Centrifuge J-26 XPI, Beckman Coulter, USA) twice at 7200rpm for 15minutes, the supernatant was collected and reserved at 4°C for further purification.

2.3 Purification of the extract

2.3.1 Diafiltration with hollow-fiber membrane contactor

Diafiltration mode was employed for purification of the extract in a hollow-fiber membrane contactor.

The setting was comprised of a feed tank, connected to a water bath (Julabo, 200F) to maintain the temperature, a water vessel, a deposit to collect the permeate, the membrane module, two peristaltic pumps, one (Reglo-Z Digital, Ismatec) connecting the water vessel to the feed tank and another (Watson Marlon 520S IP31) connecting the feed tank to the membrane unit, another pump connecting the permeate from the membrane and the permeate deposit and three manometers one (MFI6304001V, TrΔle) in the feed inlet of the membrane, another (MFI6304001V, TrΔle) in the outlet of the retentate and the last one (PCE-28, Aplisens) in the outlet of the permeate. The whole setting is represented in Figure 2.1

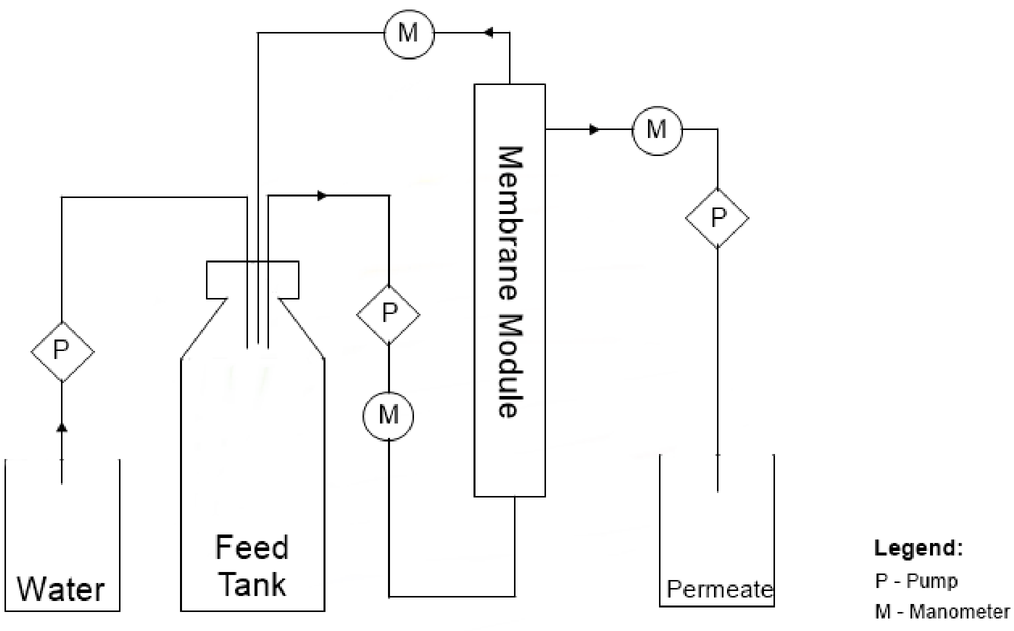

Figure 2.1: Setting of the diafiltration process employed in this work.

Before each diafiltration process hydraulic permeability was measured. After the process the membrane was cleaned by the following procedure: an aqueous solution of alkaline Ultrasil 110 0.5% (w/v) was recirculated for 30minutes, followed by an aqueous solution of acid Ultrasil 75 0.03% (v/v) also recirculated for 30minutes and finally ethanol in a concentration of 70% (v/v), recirculated during 20minutes. After each recirculation, the membrane was washed with deionized water until the pH was close to 7. After the cleaning procedure hydraulic permeability was once again measured.

2.3.2 Operation conditions

The ultrafiltration process was operated in continuous diafiltration mode, with feed volume remaining constant. It was carried at a constant temperature (40ºC), Reynolds number (129 and 267), and with controlled permeate flux, until a final diavolume of 10. (Serra *et al.*, 2020)

The mass of each diavolume was measured with a scale (PLS 8000-2A, Kern) connected to the software BioCTR. With the data collected, it was possible to plot the weight of the permeate versus the time, in which the slope corresponds to the flowrate of the permeate. The flux of permeate (J_{perm}) was then calculated with Equation 2.1:

$$J_{perm} = \frac{Q_{perm}}{A_m} \qquad \text{(Equation 2.1)}$$

Where J_{perm} is the flux of permeate ($L \cdot h^{-1} \cdot m^{-2}$), Q_{perm} is the flowrate of permeate ($L \cdot h^{-1}$) and A_m is the membrane area (m^2).

The pressure of the permeate was measured with a digital manometer (PCE-28, Aplisens) and collected by software Tera Term, while the pressures in the inlet and outlet of the membrane module were measured with analogic manometers throughout the purification process. The transmembrane pressure (TMP) was then calculated with Equation 2.2:

$$TMP = \left(\frac{P_{in}+P_{out}}{2}\right) - P_{perm} \qquad \text{(Equation 2.2)}$$

Where *TMP* is the transmembrane pressure (bar), P_{in} is the pressure in the inlet of the module, P_{out} is the pressure in the outlet of the module and P_{perm} is the pressure in the permeate.

In order to calculate the hydraulic permeability loss (Equation 2.3) for each process, hydraulic permeability was measured before and after each experiment.

$$HPL = \left(1 - \frac{L_{pf}}{L_{pi}}\right) \times 100 \qquad \text{(Equation 2.3)}$$

Where *HPL* is the hydraulic permeability loss (%), L_{pf} is the hydraulic permeability after the purification process and L_{pi} is the hydraulic permeability before the purification process.

Finally, the average permeability of the process was calculated using Equation 2.4:

$$L_{p(avg)} = \frac{J_{perm}}{TMP} \qquad \text{(Equation 2.4)}$$

Where $L_{p(avg)}$ is the average permeability ($L \cdot h^{-1} \cdot m^{-2} \cdot bar^{-1}$), J_{perm} is the permeate flux ($L \cdot h^{-1} \cdot m^{-2}$) and *TMP* is the transmembrane pressure (bar).

To study the evolution of the process in terms of salt and phenolic compounds concentration, samples of approximately 2.5mL were collected from the feed, instant and cumulative permeate at the end of each diavolume. The concentration values were obtained by measuring the conductivity for salts and absorbance at 280nm for phenolic compounds of each sample and using a calibration curve, with NaCl for conductivity and ferulic acid for absorbance.

2.4 Characterization of the extract

2.4.1 Determination of viscosity

The viscosity of the raw material was measured in a rheometer (HAAKE MARS Modular Advanced Rheometer System, Thermo Scientific), with a cone plate geometry (C35 2º Ti) and a gap of 0.105 mm, and a Peltier system to control the temperature. The dilution degrees tested were 1:1, 1:2, 1:3, 1;4, 1:8 and 1:12 at 40°C.

2.4.2 Quantification of salts present in solution

The conductivity of each sample collected was measured in a conductivity meter (Sension + EC7, Hach). It was chosen as ionic compound of reference NaCl since the cation Na^+ is present in the alkaline extract. The calibration curve was built with different concentrations of sodium chloride (≥99.5%, Honeywell): 10, 5, 2.5, 2, 1.25, 6.27×10^{-1}, 3.13×10^{-1}, 1.57×10^{-1}, 7.84×10^{-2}, 3.92×10^{-2}, 1.96×10^{-2}, 9.79×10^{-3}, 4.90×10^{-3}, 2.45×10^{-3}, 1.22×10^{-3} and 0g/L and it can be seen in Appendix A.1 (a) and (b).

2.4.3 Quantification of phenolic compounds in solution

The absorbance of each sample was measured at 280nm in a quartz cuvette (light path of 10mm, Hellma Analytics) and using a spectrophotometer (Evolution 201, Thermo Scientific). It was chosen ferulic acid as phenolic compound of reference since it’s been reported as one of the most abundant compounds in these types of extracts. (Rose, Inglett and Liu, 2010) The calibration curve was built with different concentrations of ferulic acid (≥99%, Sigma-Aldrich): 3.13×10^{-2}, 1.56×10^{-2}, 7.81×10^{-3}, 3.91×10^{-3}, 1.95×10^{-3}, 9.77×10^{-4}g/L and it’s presented in Appendix A.2.

2.4.4 Determination of dry weight (total) and ashes

To determine de total dry weight (DW_{total}, mg/mL) of the raw and purified extract, porcelain crucibles were left in the oven at 100°C for 1h, then in a desiccator until room temperature and finally, weighted (m_1, g). 10mL (v_a, mL) of the liquid was added to the porcelain crucible and left in the oven at 100°C for 24h, it was then transported to a desiccator until room temperature and weighted (m_2, g).

$$DW_{Total} = \frac{m_2 - m_1}{v_a} \times 10^{-3} \qquad \text{(Equation 2.5)}$$

To determinate the ash content (mg/mL), the crucible was left in the muffle at 550°C for 2h, cooled in the desiccator and weighted (m_3, g).

$$Ashes = \frac{m_3 - m_1}{v_a} \times 10^{-3} \qquad \text{(Equation 2.6)}$$

2.4.5 Determination of molecular weight by Gel Permeation Chromatography/Size Exclusion Chromatography (GPC/SEC)

Determination of molecular weight of raw and purified extract was performed by Gel Permeation Chromatography/Size Exclusion Chromatography (GPC/SEC), following the procedure from (Paz-Samaniego *et al.*, 2015) with slight modifications.

The separation was performed at 38ºC in a system of two columns in serie (Phenomenex PolysepGFC P5000 and Phenomenex Polysep GFC P3000, both 300x7.8 mm). For detection, a Refractive Index detector was used. As calibration pullulans in the range of Mp 6300-642000Da was used, without corrections.

2.5 Preservation of the purified extract

After the diafiltration process the purified extract was collected and kept at 4°C. It was then frozen and later freeze dried. The lyophilized product had an aspect of fiber (Figure 2.2) and it was preserved in vacuum sealed plastic bags and frozen at -20°C.

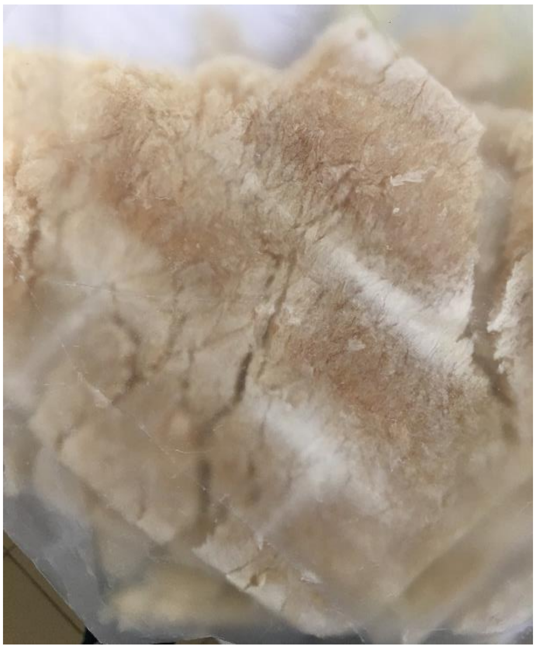

Figure 2.2: Freeze dried purified extract.

2.6 Decolorization of the purified extract

To study the decolorization of arabinoxylan, two methods were employed: adsorption by activated charcoal and hydrogen peroxide.

Activated charcoal method: (Sessa and Palmquist, 2009; Shao *et al.*, 2020)

A solution of arabinoxylan at 2% (w/v) was prepared, and 0.5% or 2% (w/v) of activated charcoal was added. The solution was stirred for 1h or 24h, at room temperature, and then filtered.

Hydrogen peroxide method: (Shi, 2016)

Solutions of arabinoxylan at 0.8% and 2% (w/v) were prepared. The solution was heated to 45°C and 10 or 20% (v/v_{final}) of hydrogen peroxide was added. The solution was left at 45°C for 2h or 5,5h with stirring. After this time the solution was concentrated and precipitated or directly precipitated in ethanol and dried.

To analyze of the evolution of the color in the solution, absorbance scans were measured before and after adding the activated charcoal or hydrogen peroxide.

2.7 Preparation of film solution

A solution of arabinoxylan at 2% (w/v) (Stoklosa *et al.*, 2019) was prepared, plasticizer (glycerol 30% ($w/w_{dry\ basis}$)) was added. (Serra *et al.*, 2020) Alternatively, different cross-linkers were also added, 10% ($w/w_{dry\ basis}$)) (Zoldners and Kiseleva, 2013): malonic acid, citric acid or succinic acid. The mixture was stirred for 15min, and a volume of 10mL was cast in 50mm teflon or plastic petri dishes. These were then left at 35°C in an oven until dried and ready to peel. After peeled they were placed in glass petri dishes and left in a desiccator at room temperature.

2.8 Characterization of the films

2.8.1 Thickness

The thickness of films was measured using an electronic micrometer (Filetta, Schut Geometrical Metrology). Measurements were made in three different places in the film.

2.8.2 Solubility

Solubility was measured following the procedure from (Ferreira *et al.*, 2016) with slight modifications.

Film samples (10x10mm) were cut and dried at 50°C for 24h, in an oven. Then, weighed to obtain a dry mass (m_1, g). The samples were immersed in 5mL of deionized water with orbital stirring (Mistral Multi-Mixer, Lab-Line Instruments, Inc.) for 24h. After this time, the solution was centrifugated at 5000rpm for 5min and the liquid was discarded. The solid residue was then dried at 50°C for 24h and weighted (m_2, g).

Solubility (*S*, %) was calculated using the following Equation 2.7:

$$S = \frac{m_1 - m_2}{m_1} \times 100 \qquad \text{(Equation 2.7)}$$

2.8.3 Water Content

The water content of film samples was determined by weighing around 0.01g of the film (m_i) in triplicate and drying them at 60°C for 20h in an oven. After this time samples were weighed again (m_f). Water Content was calculated with Equation 2.8.

$$WC = \frac{m_i - m_f}{m_f} \times 100 \qquad \text{(Equation 2.8)}$$

Where *WC* is the Water Content (%), m_i is the initial mass (g) and m_f is the final mass (g).

2.8.4 Color Measurement

The color of films was measured in triplicate with a colorimeter (Chroma Meter CR-300, Minolta, Japan), using the CIELAB (or CIE L* a* b*) color system. The calibration of the colorimeter was measured against a white standard, where L*=97.21, a*=0.14 and b*=1.99, with L* being lightness (ranging from 0=black and 100=white), a* and b* being the chromaticity coordinates: a* from red (positive) to green (negative) and b* from yellow (positive) to blue (negative).

The hue (*h*°), representing the angle on the chromaticity axis, was then calculated using the following Equation 2.9: (Ly *et al.*, 2020)

$$h^{\circ} = arctan\frac{b^*}{a^*} \qquad \text{(Equation 2.9)}$$

To convert the results of hue in radians to degrees, Equation 2.10 was applied

$$h^{\circ} = arctan\frac{b^*}{a^*} \times \frac{180}{\pi}\ , for\ a^*\ and\ b^* > 0 \qquad \text{(Equation 2.10)}$$

Or Equation 2.11

$$h^{\circ} = \left(arctan\frac{b^*}{a^*} \times \frac{180}{\pi}\right) + 180\ , for\ a^* < 0 \qquad \text{(Equation 2.11)}$$

The chroma (*C**) or saturation of color, meaning the distance from the central axis, was calculated with Equation 2.12:

$$C^* = \left((a^*)^2 + (b^*)^2\right)^{\frac{1}{2}} \qquad \text{(Equation 2.12)}$$

Where *a** and *b** are the chromaticity coordinates.

In Figure 2.3, below, it’s presented a summarized scheme with the concepts mentioned above.

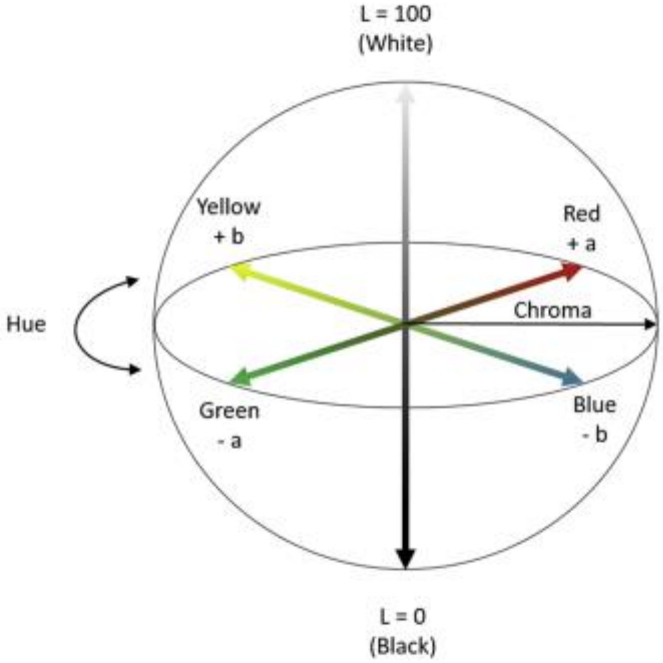

Figure 2.3: Scheme of CIELAB color system. (source: (Ly *et al.*, 2020))

Besides all of these concepts mentioned above it's also possible to calculate the color difference (ΔE^*_{ab}), which considers the changes in L*, a* and b*, between, for example, two samples, and is calculated with Equation 2.13:

$$\Delta E^*{}_{ab} = ((\Delta L^*)^2 + (\Delta a^*)^2 + (\Delta b^*)^2)^{\frac{1}{2}} \qquad \text{(Equation 2.13)}$$

Where ΔE^*_{ab} is the color difference, a^* and b^* are the chromaticity coordinates and L^* is lightness measured experimentally. If $\Delta E^*_{ab} > 1$ the color difference is observable by human eye.

2.8.5 Antioxidant Activity by Ferric Reduction Antioxidant Power (FRAP) method

FRAP reagent was prepared with 25mL of acetate buffer 0.3M, pH=3.6, 2.5mL of TPTZ (2,3,5-triphenyltetrazolium chloride) solution 10mM in HCl 40mM and 2.5mL of ferric chloride 20mM. In a test tube, 270µL of deionized water, 2.7mL of FRAP reagent and around 2mg of film sample were added. The mixture was homogenized in a vortex and incubated at 37°C in a water bath (Precision, Thermo Scientific) for 30min.

After this time the solutions were diluted in a proportion of 1:3 and the absorbance were measured at λ=595nm (Cary 100 UV-Vis, Agilent Technologies). A standard curve was obtained with different concentrations of Trolox and it's presented in Appendix A.3. The measurement was carried out in triplicate.

2.8.6 Tensile Tests (Perforation)

Perforation tests were carried in a texturometer (TA-XT-plus, Stable Micro System). Samples were fixed with tape in a support with a 1cm diameter hole in the middle. A cylindric probe with 2mm of diameter, moving at a constant velocity of 1mm/sec was used to measure the force necessary to perforate the sample.

The sample data obtained includes the force necessary to perforate the sample (perforation force, F_p) versus time and distance. Using the perforation force, it's possible to calculate the tension of perforation, σ_p (Pa), with the following Equation 2.14

$$\sigma_P = \frac{F_P}{A_c} \qquad \text{(Equation 2.14)}$$

Where F_p is the perforation force (N) and A_c is the circular area of the probe (m^2)

Considering that the film behaves in a similar way as represented in Figure 2.4 while it's being deformed.

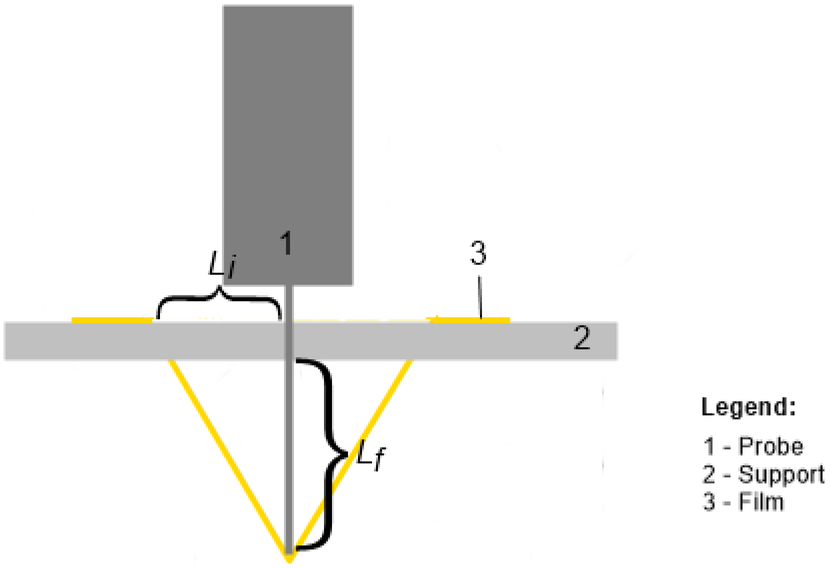

Figure 2.4: Scheme of a perforation test.

We can calculate *L* (mm) that represents the stretching of the film in the perforation, using L_i (mm) and L_f (mm) as shown in the image above (Figure 2.4), and Equation 2.15

$$L = \sqrt{(L_i)^2 + \left(L_f\right)^2} \qquad \text{(Equation 2.15)}$$

With this result we can then calculate the deformation in the perforation, ε, with Equation 2.16

$$\varepsilon = \frac{L-L_i}{L_i} \qquad \text{(Equation 2.16)}$$

Where ε is the deformation in the perforation, *L* (mm) is the stretching length in the perforation and L_i is the initial length (mm).

3. Results and Discussion

3.1 Viscosity

In order to find the appropriate dilution degree of the raw extract for further purification processes, viscosity was measured at 40°C. A previous arabinoxylan extract was referred to have an apparent viscosity of 1.8×10^{-3} Pa·s, at 40°C (Serra *et al.*, 2020), so the minimum dilution rate was chosen according to this value. In Figure 3.1 it's presented plots of apparent viscosity at each dilution degree versus the shear rate at 40°C.

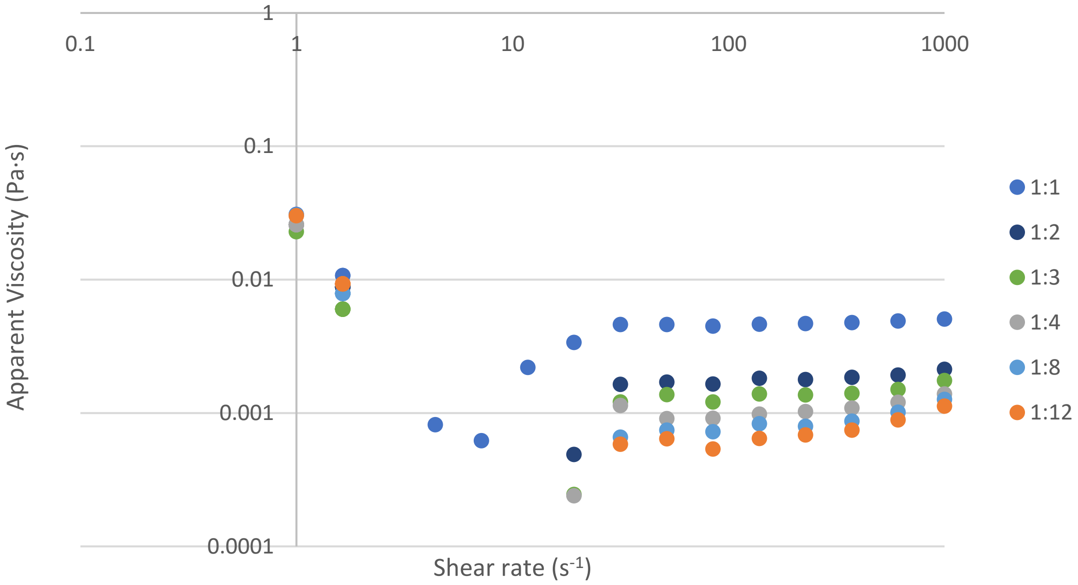

Figure 3.1: Apparent viscosity (Pa.s) in function of shear rate (s^{-1}) of the different dilution of raw extract.

The minimum dilution rate chosen was 1:2, with a value of apparent viscosity of 1.6×10^{-3} Pa·s, at 40°C, temperature in which the purification process proceeded.

3.2 Purification Process

3.2.1 Purification of the diluted raw material by dia-ultrafiltration

Since the biopolymer is very viscous at high concentrations, continuous diafiltration was employed instead of concentration mode for the purification process.

Diluted raw material was purified by dia-ultrafiltration at two different Reynolds number at the feed compartment (129 and 267). Other operation conditions like temperature and diavolume were optimized in previous works. (Serra *et al.*, 2020) To evaluate the process various parameters were calculated, such as hydraulic permeability loss, transmembrane pressure, average permeability, rejection and removal of small contaminants expressed in NaCl and Ferulic Acid equivalents.

The purification process of the extract was proceeded at two different Reynolds number (129 and 267), with controlled temperature and permeate flux.

Table 3.1, below, presents a summary containing the hydraulic permeability loss, the transmembrane pressure (TMP), flux (J_{perm}), and average permeability for the experiments at Reynolds number of 129 and 267 and their respective temperatures.

Table 3.1: Table of conditions of operation (Temperature (ºC), Hydraulic permeability loss (%), TMP (bar), J_{perm} ($L \cdot h^{-1} \cdot m^{-2}$) and average permeability ($L \cdot h^{-1} \cdot m^{-2} \cdot bar^{-1}$)) at Reynolds of 129 and 267.

Reynolds Number	Temperature (°C)	Hydraulic permeability loss (%)	TMP (bar)	J_{perm} ($L \cdot h^{-1} \cdot m^{-2}$)	Average permeability ($L \cdot h^{-1} \cdot m^{-2} \cdot bar^{-1}$)
129	40 ± 1	59 ± 12	0.31 ± 0.03	19 ± 1	62.2 ± 0.4
267	41 ± 1	82 ± 6	0.57 ± 0.03	26 ± 1	44.9 ± 3.5

Low values of hydraulic permeability loss indicate that the membrane experienced less fouling (accumulation of unwanted contaminants in the membrane), which is desired. Likewise, the values of rejection are also desirably low. On the other hand, the average permeability and percentage of removal of small contaminants are preferably high, as an indication of a good quality purification method. (Serra *et al.*, 2020)

A higher Reynolds number implies an improvement on the hydrodynamics within the system, consequently it is expected that permeate flux will also increase. As seen in the table above, we can confirm this phenomenon, where increasing the Reynolds number led to a higher permeate flux (J_{perm}). This also impacted the hydraulic permeability loss and the TMP, both rising with higher Reynolds number, this change is mainly due to an increase of membrane fouling.

Since TMP is an important factor in the hydrodynamics of the system, given that it's related to the transport process in the membrane, a higher value of TMP led to a higher permeate flux. Although, the average permeability, obtained by the ratio between permeate flux and TMP, decreased.

Other relevant factors to consider in a purification process are rejection and percentage of removal of small contaminants. Both parameters were calculated relative to NaCl and Ferulic Acid (FA) equivalents (Figures 3.2 and 3.3).

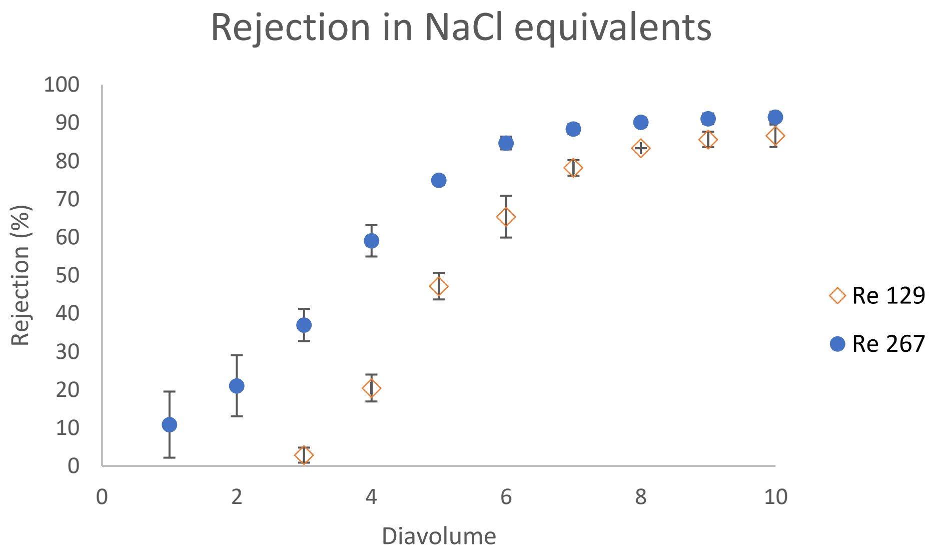

Figure 3.2: Rejection(%) in function of diavolume in equivalents of NaCl.

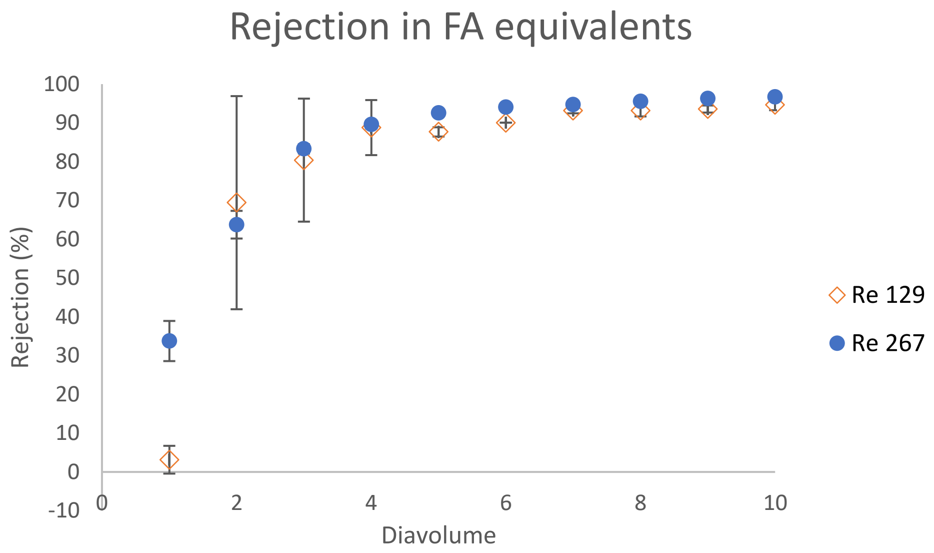

Figure 3.3: Rejection(%) in function of diavolume in equivalentes of FA.

Figures 3.2 and 3.3 shows how the apparent rejection factor evolved at each diafiltration volume, relative to NaCl and FA equivalents, respectively.

At Reynolds of 267, the apparent rejection was higher in both cases (NaCl and FA equivalents), meaning that the membrane rejected more the solute than at Reynolds of 129.

Figures 3.4 and 3.5 present how the percentage of removal of small contaminants evolved at each diafiltration volumes in NaCl and FA equivalents, respectively.

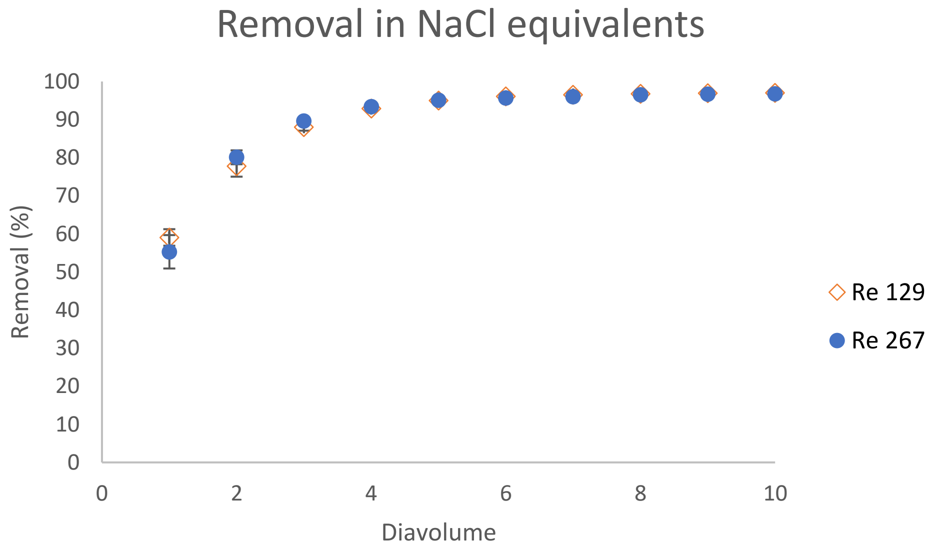

Figure 3.4: Removal(%) in function of diavolume in equivalents of NaCl.

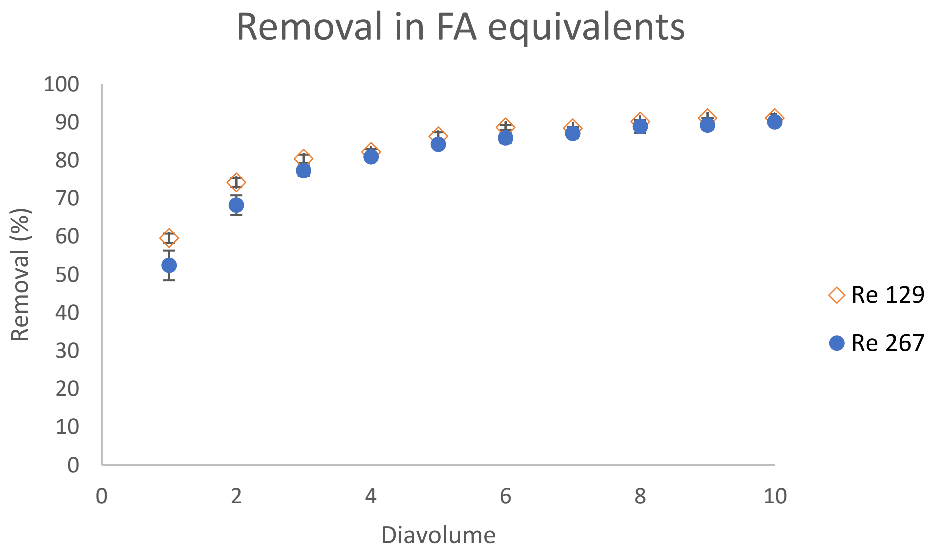

Figure 3.5: Removal(%) in function of diavolume in equivalents of FA.

By analyzing the graphics, we can denote that the percentage of removal of small contaminants was very similar at the two different Reynolds numbers, throughout the purification process.

This way, even though the process at Reynolds of 267 experiences a higher membrane fouling, corroborated by the higher values of hydraulic permeability loss and transmembrane pressure, as well as, higher apparent rejection values, the process has also a higher permeate flux, making it more productive and faster.

3.2.2 Dry weight (total) and ashes

Total dry weight and ashes of raw and purified material were determined. The values obtained are presented in the Table 3.2, below:

Table 3.2: Table of total dry weight and ashes (mg/mL) of raw extract and purified extract.

	Raw extract	Purified extract
Total dry weight (mg/mL)	40.7±0.7	12.9±0.2
Ash (mg/mL)	16.8±0.2	0.4±0.1

The total dry weight and ash content in the purified extracted is much lower than in the raw extract, indicating that the purification process was successful at removing components from the initial extract.

3.2.3 Molecular weight

Molecular weight of raw and purified extract was determined by GPC/SEC, results are presented in Table 3.3, below, and chromatograms can be found in Appendix A.4 and A.5.

Table 3.3: Table of retention time (RT) at peak (min), average molecular weight at peak (Mp, kDa), average molecular weight in number (Mn, kDa), average molecular weight in weight (Mw, kDa) and polydispersity (Mw/Mn or PD) of raw and purified extract at each peak.

		RT at peak (min)	Mp (kDa)	Mn (kDa)	Mw (kDa)	Mw/Mn or PD
Raw Extract	Peak 1	26.95±0.03	46.8±0.8	68.3±0.9	127.0±2.8	1.85±0.02
	Peak 2	32.77±0.05	2.0±0.1	2.1±0.1	2.5±0.1	1.14±0.01
Purified Extract	Peak 1	24.06±0.02	225.1±2.9	156.4±7.5	263.9±0.3	1.69±0.08
	Peak 2	30.54±0.13	6.6±0.4	5.1±0.4	6.0±0.3	1.17±0.04

The purified extract has lower retention times and less dispersed populations. While the raw extract presents various dispersed populations, which are not very well resolved and can contribute to error. This may explain the difference in molecular weight between the two extracts.

The different behavior of each sample may be due to their own intrinsic characteristics, for example the viscosity greatly influences the velocity of the elution and consequently the retention time.

3.3 Decolorization of the arabinoxylan extract

3.3.1 Activated charcoal adsorption method

Arabinoxylan was decolorized with activated charcoal at two different concentrations (0.5 and 2% ($w_{\text{activated charcoal}}/v_{\text{solution}}$)) for 1h. Spectra were measured before and after the addition of the activated charcoal (Figures 3.6 and 3.7)

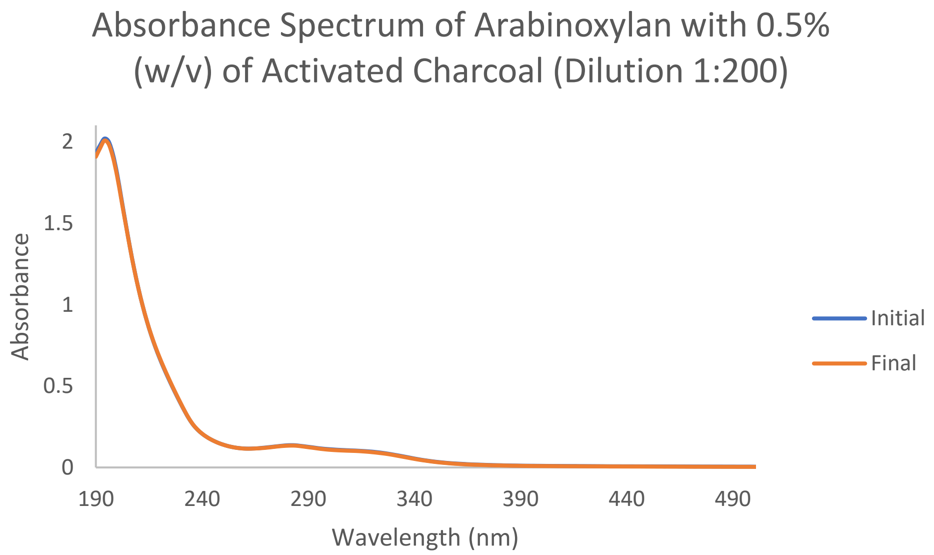

Figure 3.6: Overlap of absorbance spectrum of arabinoxylan with 0.5% (w/v) of activated charcoal before (blue) and after 1h of contact (orange) in a dilution rate of 1:200.

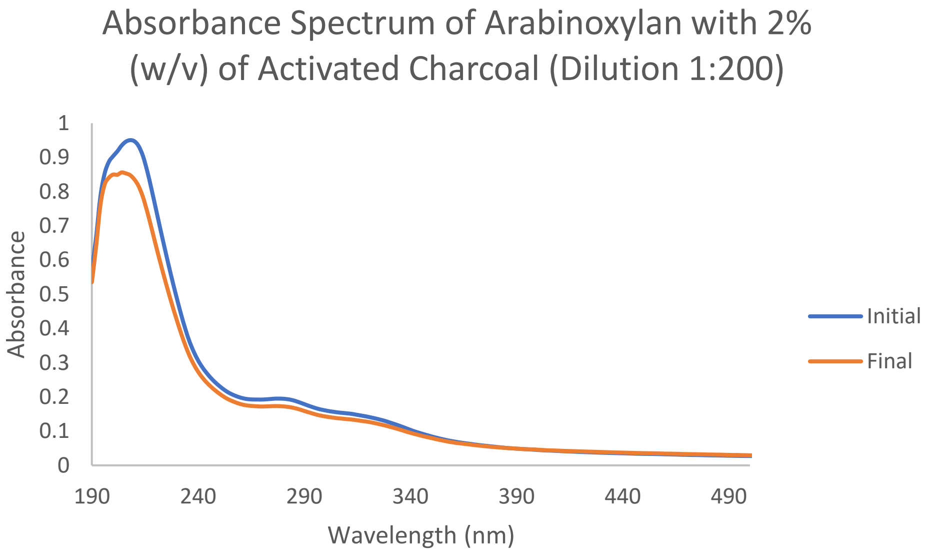

Figure 3.7: Overlap of absorbance spectrum of arabinoxylan with 2% (w/v) of activated charcoal before (blue) and after 1h of contact (orange) in a dilution rate of 1:200.

The spectrum of the solution with 2% (w/v) of activated charcoal, unlike the spectrum with 0.5% (w/v), shows a decrease in absorbance at around 210nm and around 280nm, meaning that the charcoal was able to adsorb some components of the solution, however, only to a minor extent. This difference in the solution with 2% (w/v) of activated charcoal is not noticeable at the naked eye since the solution appears to not have changed. (Figure 3.8)

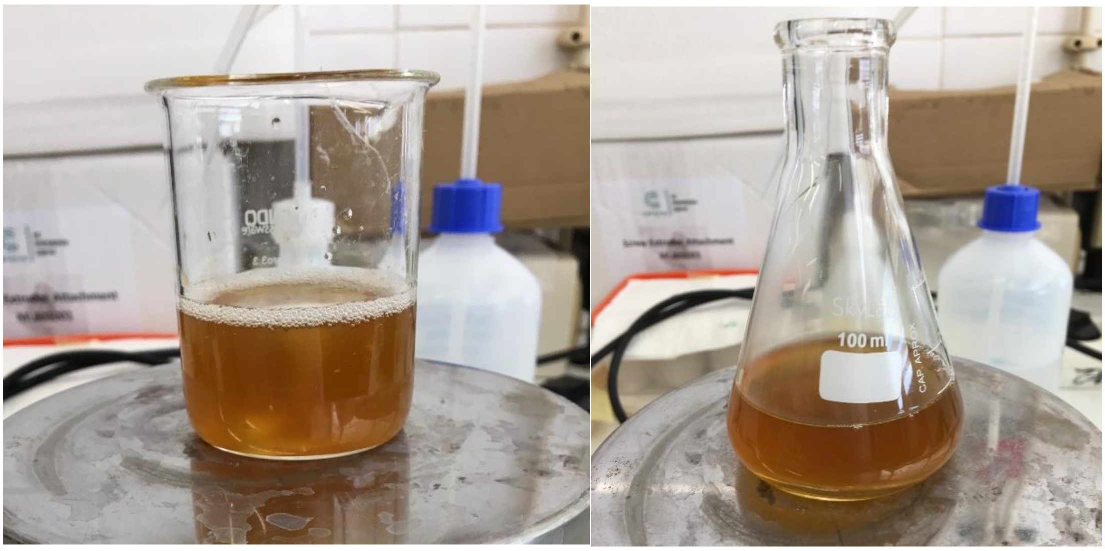

Figure 3.8: Solution of arabinoxylan before the addition of activated charcoal (left) and filtered after the reaction time of 1h (right).

Additionally, a decolorization test was done with 2% (w/v) of activated charcoal for 24h. However, both the final filtrated solution and the absorbance spectrum (Figure 3.9) obtained didn't show much difference from previous results.

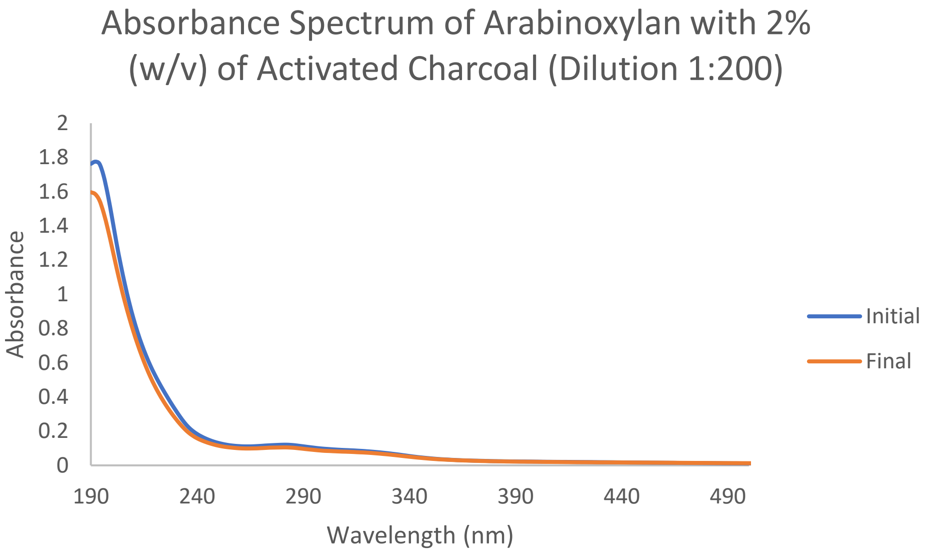

Figure 3.9: Overlap of absorbance spectrum of arabinoxylan with 2% (w/v) of activated charcoal before (blue) and after 24h of contact (orange) in a dilution rate of 1:200.

Therefore, this decolorizing method doesn't seem to be ideal for the arabinoxylan extract since it's not selective and doesn't produce a visible change in the color of the solution.

3.3.2 Hydrogen Peroxide method

Another method employing hydrogen peroxide was tested for the decolorization of arabinoxylan. Solutions of 0.8 and 2% (w/v) of arabinoxylan were prepared and decolorized using hydrogen peroxide in a concentration of 10% (v/v_{final}). Absorption spectra were measured before and after the addition of peroxide and are presented below (Figures 3.10 and 3.11)

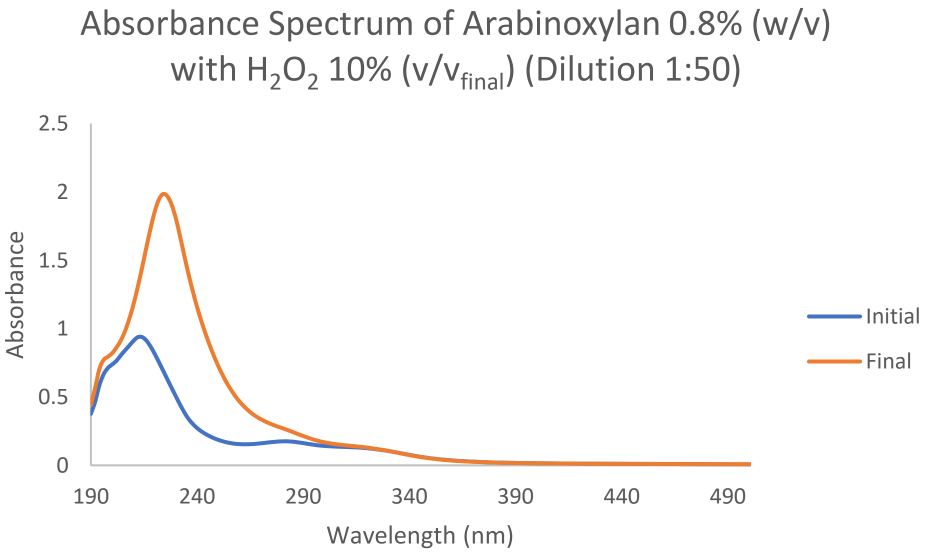

Figure 3.10: Overlap of absorbance spectrum of arabinoxylan 0.8% (w/v) with 10% (v/v_{final}) of hydrogen peroxide before (blue) and after 2h of reaction time at 45ºC (orange) in a dilution rate of 1:50.

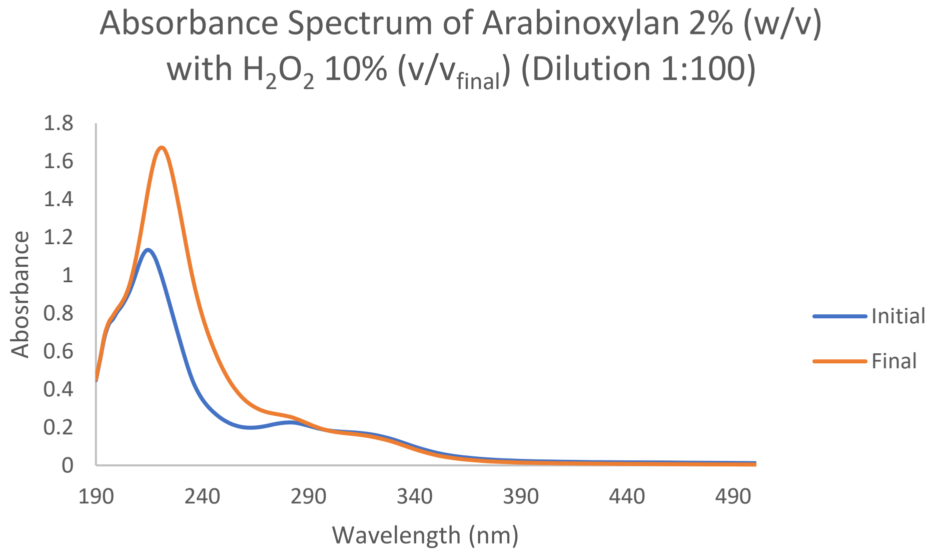

Figure 3.11: Overlap of absorbance spectrum of arabinoxylan 2% (w/v) with 10% (v/v_{final}) of hydrogen peroxide before (blue) and after 2h of reaction time at 45ºC (orange) in a dilution rate of 1:100.

By analyzing the spectrums it's difficult to conclude how the solution might have changed during the decolorizing process, due to the presence of a higher absorbance around 220nm after the experiment time. The higher absorbance around 220nm after the decolorizing process is due to the presence of hydrogen peroxide. This presence also shifted the maximum peak from 210nm to 220nm, since hydrogen peroxide presents a maximum absorbance at 230nm (absorbance spectrum in Appendix A.6)

However, at the naked eye the addition of hydrogen peroxide originated a much lighter solution. (Figure 3.12)

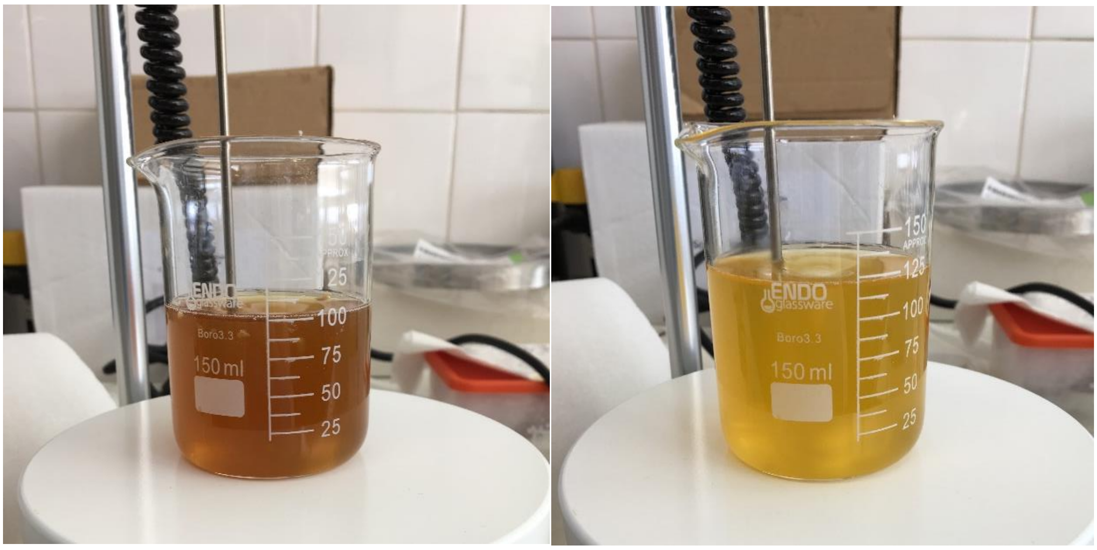

Figure 3.12: Solution of arabinoxylan before the addition of hydrogen peroxide (left) and after the reaction time of 2h at 45ºC (right).

The original solution (left), is much darker and brownish, while the solution after the decolorization process (right) is lighter and yellow.

Additionally, different reaction times and peroxide concentrations were tested.

For peroxide concentration 20% (v/v_{final}) was used in the decolorizing process (Figure 3.13).

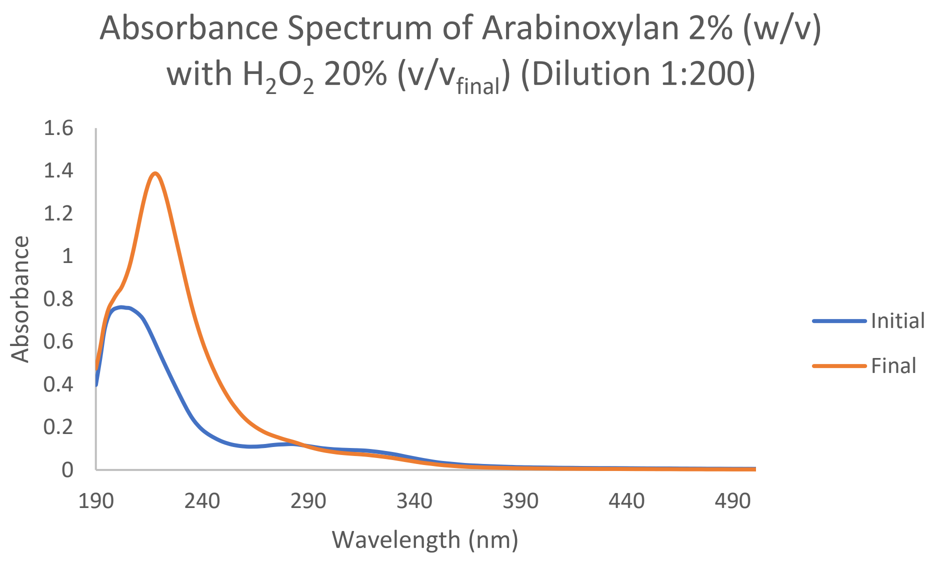

Figure 3.13: Overlap of absorbance spectrum of arabinoxylan 2% (w/v) with 20% (v/v$_{final}$) of hydrogen peroxide before (blue) and after 2h of reaction time at 45ºC (orange) in a dilution rate of 1:200.

For experiment time, 5,5h was tested instead of the initial 2h (Figure 3.14).

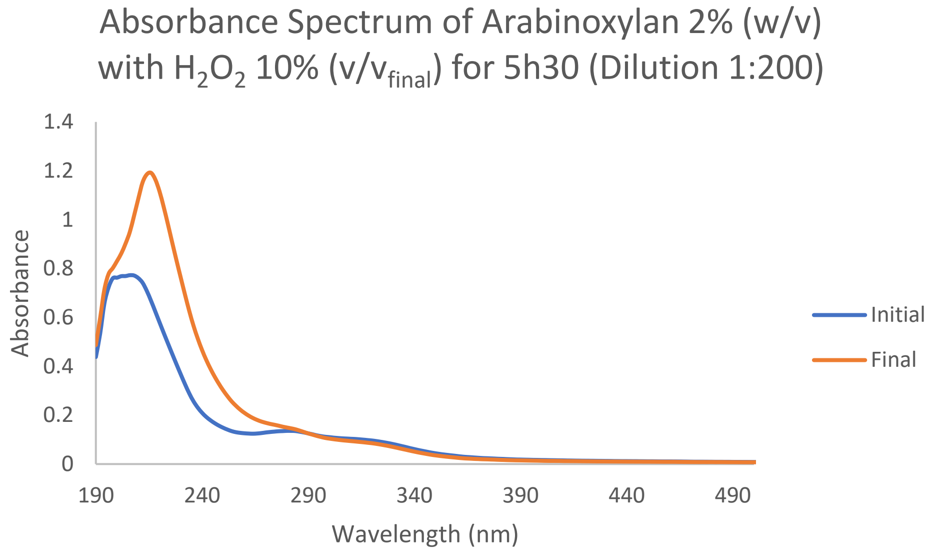

Figure 3.14: Overlap of absorbance spectrum of arabinoxylan 2% (w/v) with 10% (v/v$_{final}$) of hydrogen peroxide before (blue) and after 5h30 of reaction time at 45ºC (orange) in a dilution rate of 1:200.

In both cases no significant difference in color or absorbance spectrum was seen. Therefore, the decolorizing process with hydrogen peroxide proceeded without additional changes.

3.3.3 Optimization of decolorization method

It was found that precipitating arabinoxylan from decolorized solutions by adding ethanol was difficult due to the low concentration of arabinoxylan in the solution. Attempts at concentrating the solution by evaporating the solvent were also not optimal since they were very time-consuming.

Since the purpose of this step would be only to recover the arabinoxylan in solution in order to solubilize it again for film-forming solutions, it was decided to skip the precipitation step and prepare solutions for decolorization in the same concentration that the film-forming solution would have (2%(w/v)).

3.4 Film-forming solutions and resulting films

Solutions of arabinoxylan (2%(w/v)) were prepared and decolorized according to the optimized hydrogen peroxide method. After the 2h of decolorization, plasticizer (glycerol) and cross-linker (citric acid, malonic acid or succinic acids) were added. Details are presented in the Table 3.4 below.

Table 3.4: Every different formulation tested of arabinoxylan films. For the decolorization process it was used hydrogen peroxide 10%(v/vfinal) for 2h at 45ºC.

Film Ax 2%(w/v)	Glycerol (30% $w/w_{dry\ basis}$)	Citric Acid (10% $w/w_{dry\ basis}$)	Succinic Acid (10% $w/w_{dry\ basis}$)	Malonic Acid (10% $w/w_{dry\ basis}$)	Sodium Hypo-phosphite (50% w/w_{acid})	NaOH (1M)	Decolo-rized film
1							
2	x						
3							x
4	x						x
5	x		x				x
6	x			x			x
7	x	x					x
8	x	x				x until pH=6	x
9	x	x			x		x
10 Additional drying at 90°C, 1h	x	x					x

The addition of diacids such as citric acid, malonic acid or succinic acid as cross-linking agents had the purpose of promoting an esterification reaction between the carboxylic group of the diacid and the alcohol groups present in arabinoxylan. Sodium Hypophosphite was added as catalyst for this reaction. (Zoldners and Kiseleva, 2013) NaOH was added to study how the pH may affect the reaction. Heat treatment was applied (90° for 1h) in order to observe how the film would perform and change in contact with a higher temperature. (Yang *et al.*, 2019)

After dried and peeled, films were photographed and are presented in Table 3.5 below:

Table 3.5: Arabinoxylan formulation and their respective obtained film.

Film Composition	Image
1 (Arabinoxylan)	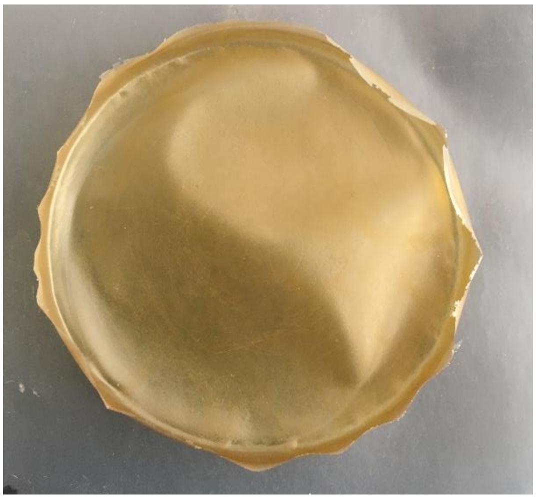
2 (Arabinoxylan+Glycerol)	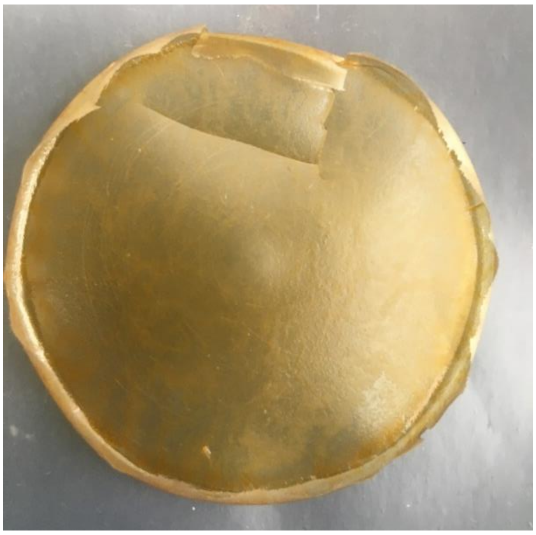
3 (Arabinoxylan+H_2O_2)	
4 (Arabinoxylan+H_2O_2+Glycerol)	
5 (Arabinoxylan+H_2O_2+Glycerol+Succinic Acid)	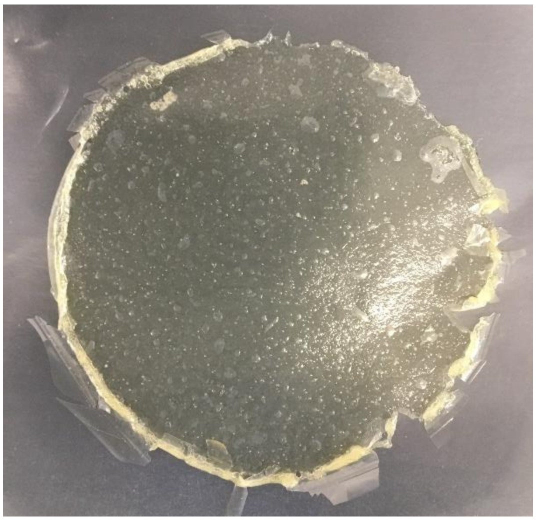

6 (Arabinoxylan+H_2O_2+Glycerol+Malonic Acid)	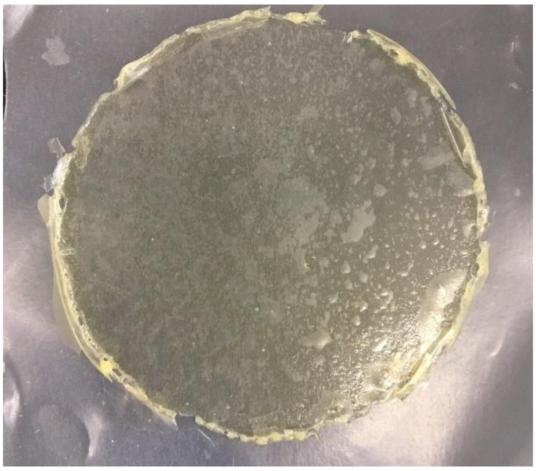
7 (Arabinoxylan+H_2O_2+Glycerol+Citric Acid)	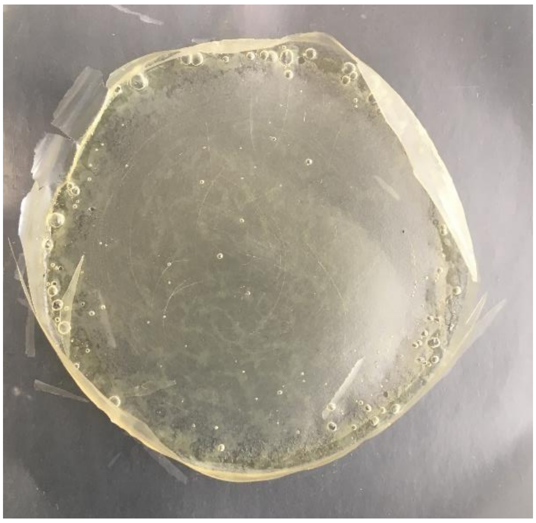
8 (Arabinoxylan+H_2O_2+Glycerol+Citric Acid+NaOH)	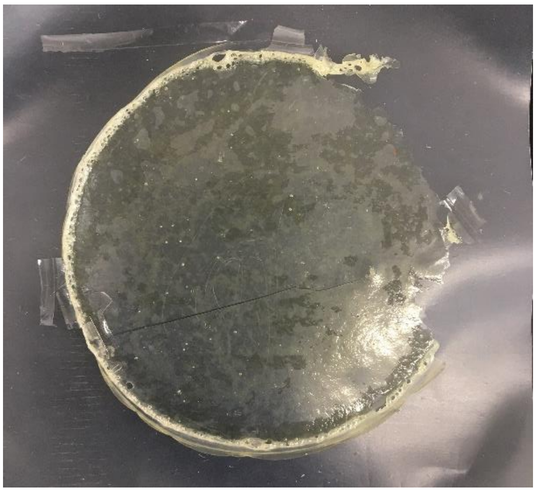

9 (Arabinoxylan+H_2O_2+Glycerol+Citric Acid+Sodium Hypophosphite)	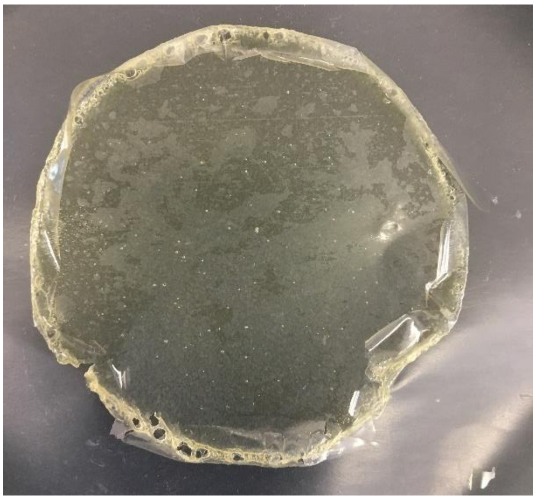
10 (Arabinoxylan+H_2O_2+Glycerol+Citric Acid+90°C for 1h)	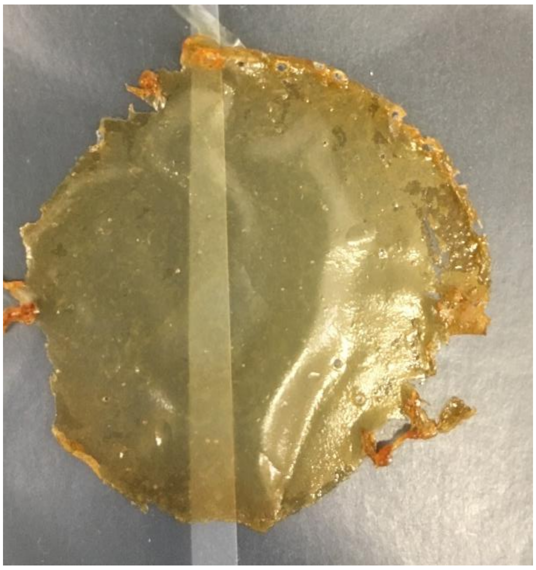

Similarly, to what was observed with the film-forming solution before and after the addition of hydrogen peroxide, films were also much lighter if the solution was decolorized when compared with films prepared without any decolorization process. Additionally, the heat treatment originated a darker film than one with the same formulation but without suffering the heat treatment.

To further compare this color difference between films and other properties, various characterization tests were performed.

3.5 Films characterization

3.5.1 Color Measurement

The color of films was measured as described in section 2.8.4 and are summarized below in Table 3.6.

Table 3.6: Values of lightness (L*), chromaticity coordinates (a* and b*) and their respective calculated hue (hº) and chroma (C*) of each arabinoxylan film.

Film	L*	a*	b*	h°	C*
1 (Ax)	80.29±0.69	0.65±0.32	43.60±1.21	89.15±0.40	43.60±1.21
2 (Ax+Glycerol)	79.65±0.99	0.56±0.48	46.85±1.90	89.33±0.57	46.86±1.91
3 (Ax+H_2O_2)	95.18±0.78	-1.91±0.75	9.87±3.45	100.85±0.46	10.05±3.53
4 (Ax+H_2O_2+ Glycerol)	95.64±0.24	-1.77±0.17	8.69±0.64	101.48±0.23	8.87±0.66
5 (Ax+H_2O_2+ Glycerol+Succinic Acid)	95.92±0.50	-1.74±0.08	9.21±0.35	100.72±0.18	9.37±0.36
6 (Ax+H_2O_2+ Glycerol+Malonic Acid)	95.50±0.39	-2.35±0.25	12.54±0.95	100.61±0.36	12.76±0.98
7 (Ax+H_2O_2+ Glycerol+Citric Acid)	94.94±0.23	-2.62±0.19	14.56±1.00	100.19±0.24	14.79±1.01
8 (Ax+H_2O_2+ Glycerol+Citric Acid+NaOH)	94.78±0.12	-2.66±0.08	13.05±0.65	101.54±0.26	13.32±0.65
9 (Ax+H_2O_2+ Glycerol+Citric Acid+Sodium Hypophosphite)	95.30±0.16	-2.29±0.08	12.62±0.23	100.27±0.19	12.82±0.24
10 (Ax+H_2O_2+ Glycerol+Citric Acid+90°C for 1h)	89.03±0.88	-1.55±0.10	28.04±1.00	93.16±0.29	28.08±0.99

As seen in Table 3.6, films that were decolorized showed a similar value of lightness (L*), which are also very close to 100, equivalent to white. Arabinoxylan films that were not decolorized showed a lower value of L* which correspond to what was observed at the naked eye, where the films show a darker color than the decolorized ones. The heat treatment originated a darker film than the original one, with the values of L* it’s noted that the lightness of this film is somewhere in between the decolorized and not decolorized ones.

By using the chromaticity coordinates, we can somewhat place these values in the CIELAB hue circle (Figure 3.15). We observe that the non decolorized films are closer to strong yellow-orange color while the decolorized films are closer to a light yellow. Once again, the film that suffered heat treatment is somewhere in between.

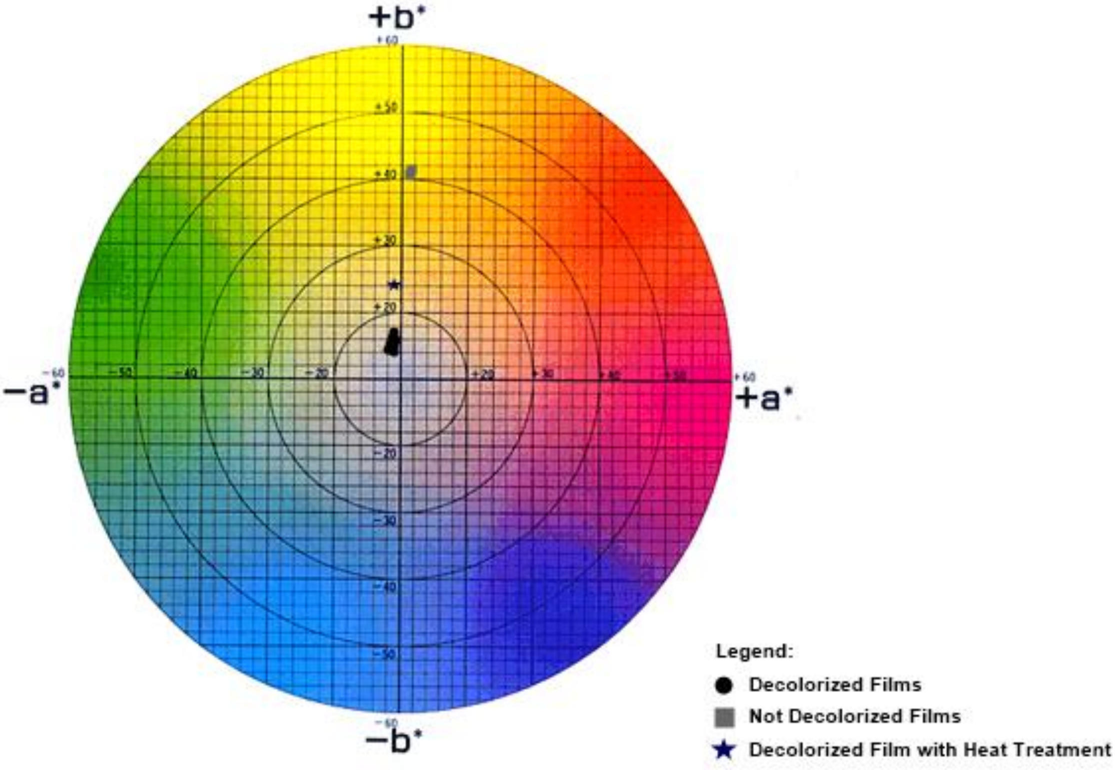

Figure 3.15: Position of each arabinoxylan film in the CIELAB color circle.

When compared to values obtained previously of arabinoxylan films (Table 3.7) (Serra *et al.*, 2020), it can be noticed a similarity between the not decolorized films in this work and the ones presented previously, which is easily justified since both films have very similar formulations.

Table 3.7: Values of lightness (L*), chromaticity coordinates (a* and b*) and their respective calculated hue (hº) (C*) of arabinoxylan film obtained in (Serra *et al.*, 2020).

Film	L*	a*	b*	h°
Ax+Glycerol 30% (w/$w_{\text{dry basis}}$)	73.55±2.98	2.50±1.05	42.54±3.35	86.64±1.28
Ax+Glycerol 30% (w/$w_{\text{dry basis}}$)+Ferulic Acid 10% (w/$w_{\text{dry basis}}$)	76.27±0.31	1.78±0.04	37.83±0.51	87.28±0.04

To further study if the color difference between decolorized, not decolorized and heat-treated films is perceptible by human eyes, color the difference between them was calculated. Results are presented in Table 3.8, below:

Table 3.8: Color difference between a not decolorized film (1) and a decolorized one (3) and between a decolorized one (7) and a heat treated one (10).

Film Samples	Color Difference (ΔE^*_{ab})
1 (Ax) & 3 (Ax+H_2O_2)	36.96±3.36
7 (Ax+H_2O_2+Glycerol+Citric Acid) & 10 (Ax+H_2O_2+Glycerol+Citric Acid+90°C for 1h)	14.75±1.34

Since it's important to be able to quantify the changes in color, instead of using adjectives and broad colors to describe them, we can simply quantify this change with ΔE^*_{ab}. Normally for food products, if the color difference is superior to 6 the change is certainly detectable by human eyes, which we can confirm with the values obtained, meaning that between the film samples measured their colors are very different.

Considering these results, it seems favorable, in terms of film color, to apply the decolorization method with hydrogen peroxide. On the other hand, the heat treatment didn't show to be advantageous since it darkened the film, therefore this method was discarded.

3.5.2 Antioxidant activity

It is known that ferulic acid presents antioxidant activity (Rose, Inglett and Liu, 2010), therefore it's expected that its presence in solution would result in a film that would also present some antioxidant activity.

To further study how the addition of hydrogen peroxide could affect the extract, antioxidant activity was measured in non-decolorized films and in a decolorized one, by FRAP method (Figure 3.16).

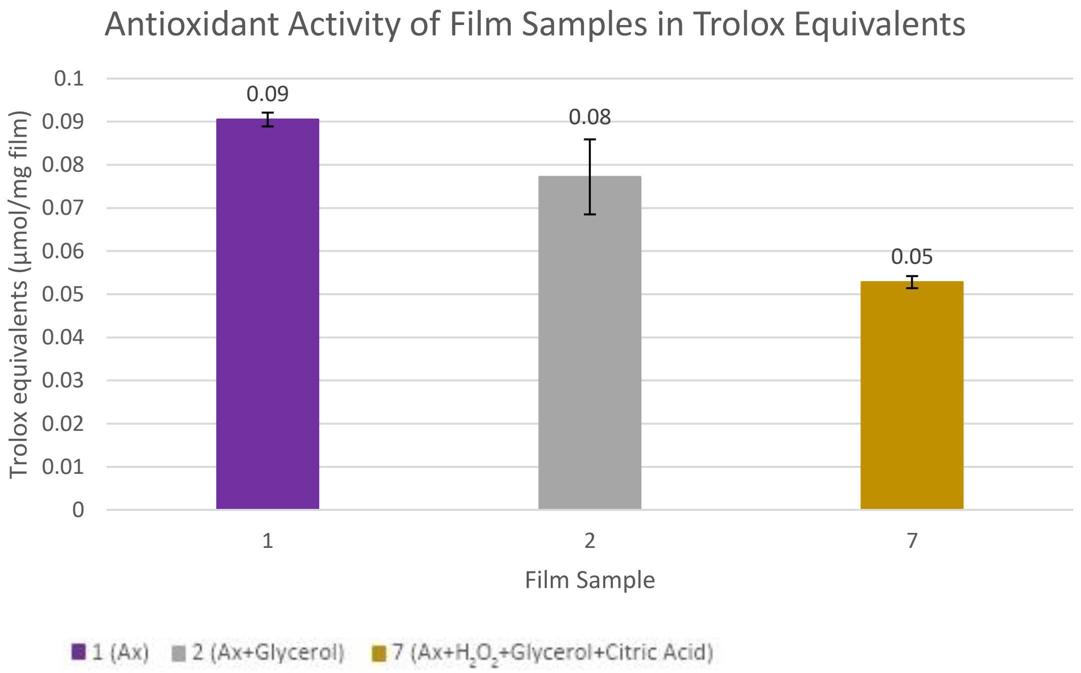

Figure 3.16: Antioxidant activity (µmol/mg film) of film samples 1, 2 and 7 in Trolox equivalents

Film 1 which is formulated with only arabinoxylan, without the addition of any extra components, shows the highest antioxidant activity. The addition of glycerol (film 2) reduced slightly the antioxidant activity of the film in relation to the pure one.

The addition of hydrogen peroxide (a strong oxidizer) and citric acid (film 7) did also reduce the antioxidant activity of the film in comparison with the pure arabinoxylan film (1), however there’s still significant activity remaining.

When compared with a similar arabinoxylan film with 30% glycerol, prepared by (Serra *et al.*, 2020), which had an antioxidant activity of 0.02µmol/mg film. The films obtained in this work all show a higher antioxidant activity, including the film that was decolorized and showed the lowest activity.

3.5.3 Solubility

Since the objective was to produce less soluble films in water, by promoting an esterification reaction, their solubility was tested.

The results are presented in Figure 3.17.

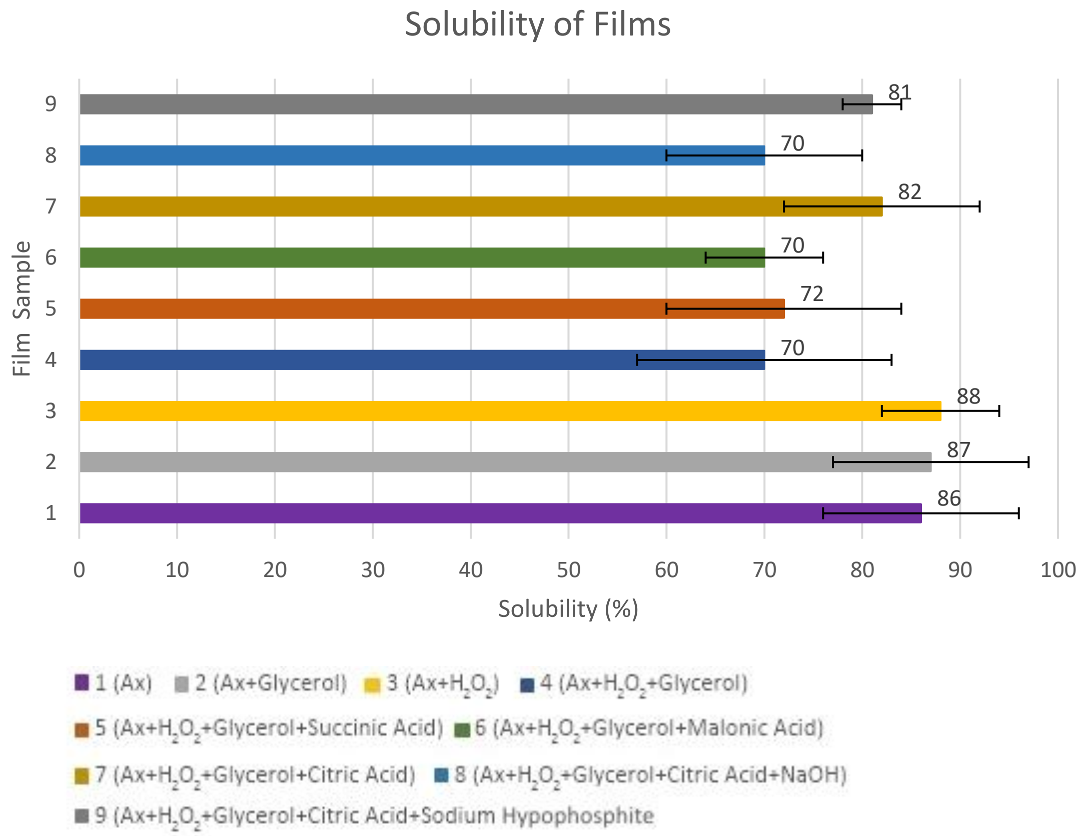

Figure 3.17: Solubility(%) of every film sample

Films 1 and 2 which didn’t suffer decolorization, showed a higher solubility than most of the decolorized ones, along with film 3 which was only decolorized.

On the other hand, we can notice that decolorized films only with plasticizer (4), and with plasticizer and one cross-linker (films 5 with succinic acid and 6 with malonic acid) showed a lower solubility, meaning this addition was advantageous to the formulation of the films.

Amongst all films, it seems that malonic acid, and citric acid together with NaOH, performed better as cross-linkers, regarding the lowest solubility values obtained.

However, it's important to mention that these values of solubility are not exceptionally different, meaning that the cross-linking process didn't occur in the extent it was desired. Possibly due to the solvent used (water), which doesn't favor the esterification reaction.

Furthermore, when compared with the solubility of other biopolymers, such as FucoPol films (47.5±5.2%) and chitosan films (30.5±0.5%) (Ferreira *et al.*, 2016), the solubility of arabinoxylan films is much higher.

3.5.4 Mechanical tests (Perforation)

Perforation tests were carried in duplicate or triplicate in film samples that could cover the whole surface necessary of the platform to carry an accurate assay. The objective of the test was to study the mechanical properties of each films, namely the tension and deformation upon perforation.

Before each test, the thickness of the film sample was measured, as well as the water content right after the assay. A summary of the values obtained can be found in Table 3.9.

Table 3.9: Thickness (mm) and Water Content (%) of film samples prepared for perforation tests

Film Sample	Thickness (mm)	Water Content (%)
1 (Ax)	0.081±0.016	7±6
2 (Ax+Glycerol)	0.098±0.002	7±2
3 (Ax+H_2O_2)	0.069±0.016	7±4
6 (Ax+H_2O_2+ Glycerol+ Malonic Acid)	0.078±0.008	7±3
7 (Ax+H_2O_2+ Glycerol+Citric Acid)	0.091±0.014	10±2
8 (Ax+H_2O_2+ Glycerol+ Citric Acid+NaOH)	0.199±0.008	8±7
9 (Ax+H_2O_2+ Glycerol+Citric Acid+Sodium Hypophosphite)	0.097±0.003	7±2

The results obtained from the perforation tests are shown in Figure 3.18 (tension upon perforation) and Figure 3.19 (deformation upon perforation).

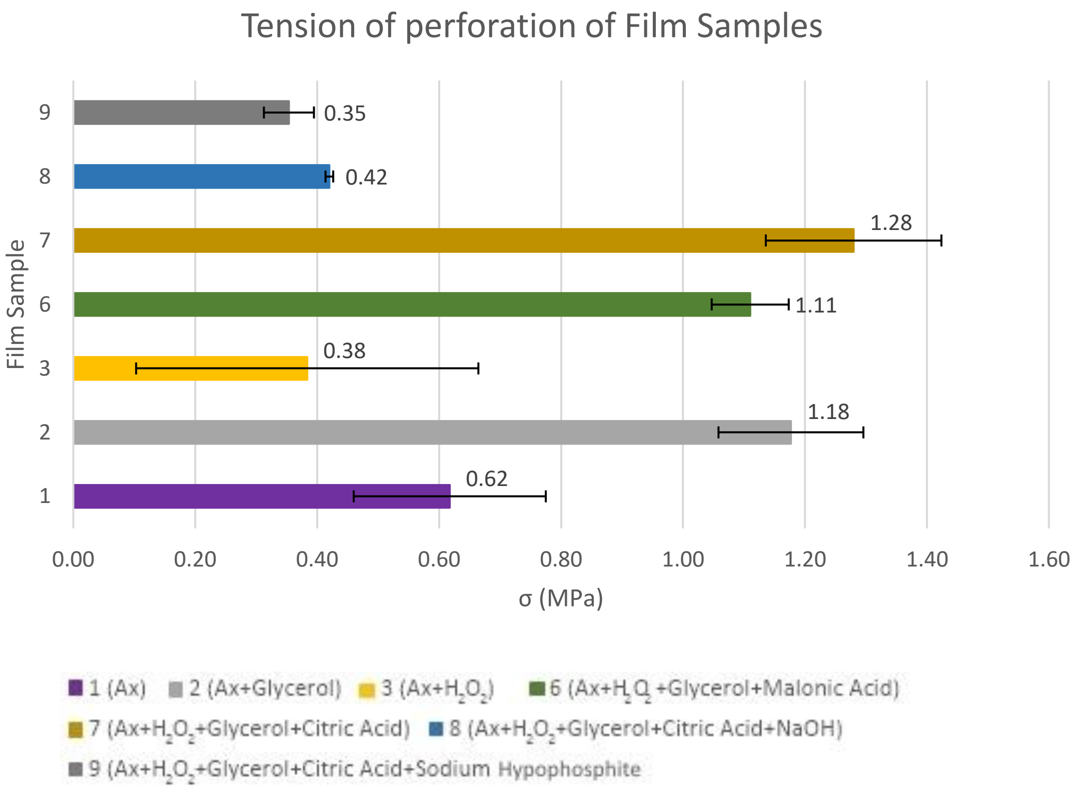

Figure 3.18: Tension of perforation (MPa) of film samples tested

When compared with the film formulated with only arabinoxylan (film 1), films 2, 6 and 7, showed a higher tension of perforation, meaning that these films present a higher mechanical resistance upon perforation than pure arabinoxylan films.

On the other hand, film 3 presented a lower tension value that may be due to the lack of plasticizer, imparting a more brittle and fragile structure. Films 8 and 9 had also a lower value of tension, attributed in these cases to the presence of NaOH and sodium hypophosphite, respectively.

A film prepared from maize bran arabinoxylan by (Anderson and Simsek, 2019b), with 25% glycerol showed a tension of perforation of (2.42±0.12)MPa, a higher value than all of the films prepared in this work (Figure 3.18). However, this film was conditioned to 50% relative humidity, meaning that its water content was also higher when compared with our films (Table 3.9), which can greatly influence the results obtained in this type of tests.

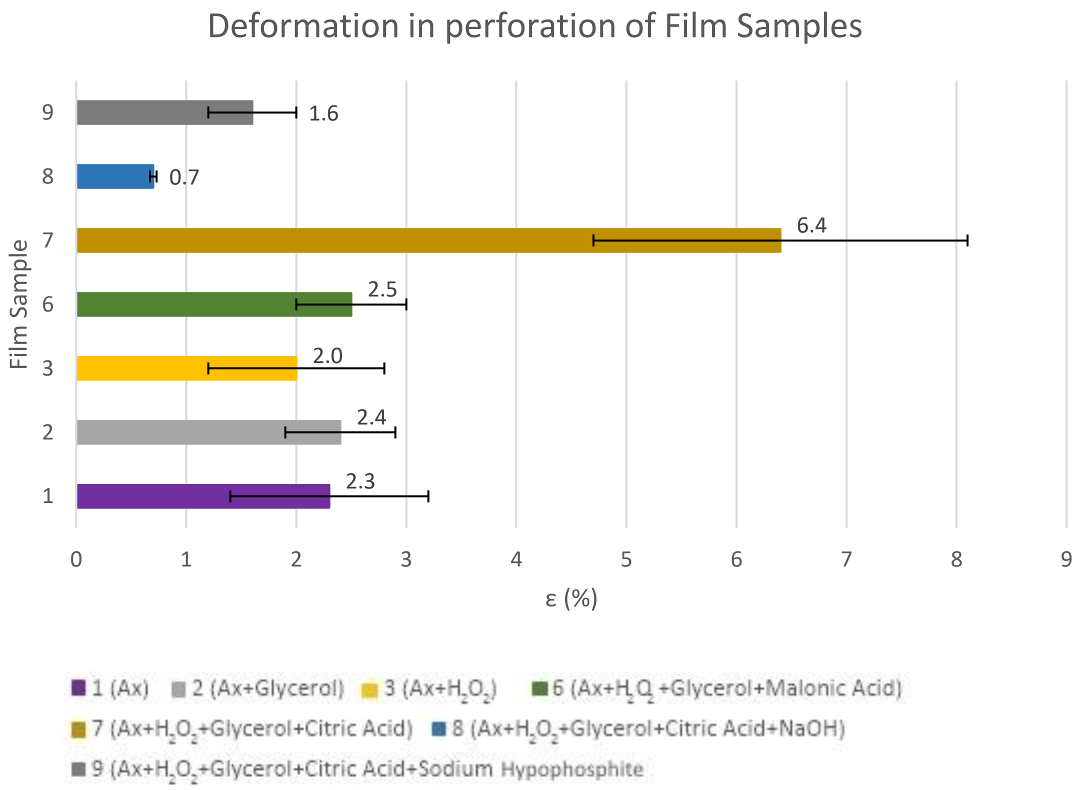

Figure 3.19: Deformation in perforation (%) of film samples tested

Film 7 suffered the highest deformation, around 6%, upon perforation, while most of the films suffered a deformation of around 2%, apart from film 8 that only was deformed 0.7%. Still, all films exhibited a small ability to elongate during perforation tests.

With the results obtained, films 2, 6 and 7, showed to have better mechanical properties. However, film 2 wasn’t decolorized. For applications were decolorization is important, films 6 and 7, are the ones with greater potential, which were formulated with glycerol as plasticizer and malonic or citric acid, respectively, as cross-linker.

4. Conclusions

Purification of raw arabinoxylan was successful by employing membrane filtration, in a hollow-fiber membrane contactor. Two different Reynolds numbers were tested: 129 and 267. At Reynolds number 267, the permeate flux and transmembrane pressure were higher, while average permeability was lower and rejection as well as hydraulic permeability loss were higher, this last parameter indicates that at a higher Reynolds number the membrane experiences more fouling than at Reynolds 129, though the process is more favorable in terms of hydrodynamics. However, since the objective of the purification was to remove small contaminants from the solution and percentages of removal were very similar at the two different Reynolds, it seems advantageous to proceed the purification at a higher Reynolds number.

Decolorizing the purified extract with hydrogen peroxide was shown to be effective in producing a lighter solution, while still retaining film-forming properties.

In terms of formulation, the addition of plasticizer (glycerol) and cross-linker (malonic acid or citric acid) seems advantageous regarding solubility and mechanical properties. Although this addition plus the decolorization process decreased the antioxidant activity of the film, there was still some significant activity present. It’s not clear if the addition of NaOH or sodium hypophosphite to the referred formulations brought major improvements in the properties of the films, since in both solubility and mechanical properties, the resulting films didn’t perform significantly better.

5. Future Work

As future work it is important to continue researching ways of optimizing the arabinoxylan extract. In terms of color, other methods could be employed such as extraction of the colored compounds with food grade solvents.

In terms of formulation of arabinoxylan films, other solvents could be tested, besides water, or other techniques, such as thermo-compression molding. Additionally, an acetylation reaction in acidic media without the presence of water could also be tested. These modifications would have as objective to create films which would be more resistant to water, meaning more insoluble.

An additional characterization can also be performed in the produced films in this thesis, namely in terms of water vapor permeability, gas permeability and mechanical properties under tensile tests.

The study of optimized arabinoxylan films in terms of applications, such as food packaging and coatings, or other applications in other fields, is also a possible future research.

6. References

Ahmed, E. M. (2015) ‘Hydrogel: Preparation, characterization, and applications: A review’, *Journal of Advanced Research*. Cairo University, 6(2), pp. 105–121. doi: 10.1016/j.jare.2013.07.006.

Anderson, C. and Simsek, S. (2018) ‘What Are the Characteristics of Arabinoxylan Gels?’, *Food and Nutrition Sciences*, 09(07), pp. 818–833. doi: 10.4236/fns.2018.97061.

Anderson, C. and Simsek, S. (2019a) ‘A novel combination of methods for the extraction and purification of arabinoxylan from byproducts of the cereal industry’, *Journal of Food Measurement and Characterization*. Springer US, 13(2), pp. 1049–1057. doi: 10.1007/s11694-018-00020-4.

Anderson, C. and Simsek, S. (2019b) ‘Mechanical profiles and topographical properties of films made from alkaline extracted arabinoxylans from wheat bran, maize bran, or dried distillers grain’, *Food Hydrocolloids*. Elsevier Ltd, 86, pp. 78–86. doi: 10.1016/j.foodhyd.2018.02.016.

Association, G. C. G. (2020) *Corn Overview*. Available at: http://georgiacorngrowers.org/corn-overview/ (Accessed: 28 November 2020).

Belgacem, M. N. and Gandini, A. (2008) *Monomers, Polymers and Composites from Renewable Resources*, *Elsevier*.

Belmokaddem, F. Z. *et al.* (2011) ‘Green synthesis of xylan hemicellulose esters’, *Carbohydrate Research*, 346(18), pp. 2896–2904. doi: 10.1016/j.carres.2011.10.012.

Broekaert, W. F. *et al.* (2011) ‘Prebiotic and other health-related effects of cereal-derived arabinoxylans, arabinoxylan-oligosaccharides, and xylooligosaccharides’, *Critical Reviews in Food Science and Nutrition*, 51(2), pp. 178–194. doi: 10.1080/10408390903044768.

Cheryan, M. (1998) *Ultrafiltration and Microfiltration Handbook*, *Ultrafiltration and Microfiltration Handbook*. doi: 10.1201/9781482278743.

Chiellini, E. (2008) *Environmentally Compatible Food Packaging*, *Woodhead Publishing Limited*. doi: 10.1533/9781845694784.2.182.

Dhineshkumar, V. and Ramasamy, D. (2017) ‘Review on Membrane Technology Applications in Food and Dairy Processing’, *Journal of Applied Biotechnology & Bioengineering*, 3(5), pp. 399–407. doi: 10.15406/jabb.2017.03.00077.

Ferreira, A. R. V. *et al.* (2016) ‘Development and characterization of bilayer films of FucoPol and chitosan’, *Carbohydrate Polymers*. Elsevier Ltd., 147, pp. 8–15. doi: 10.1016/j.carbpol.2016.03.089.

Fundador, N. G. V. *et al.* (2012) ‘Syntheses and characterization of xylan esters’, *Polymer*. Elsevier Ltd, 53(18), pp. 3885–3893. doi: 10.1016/j.polymer.2012.06.038.

Good Natured Products (2020). Available at: https://goodnaturedproducts.com/pages/eco-friendly-sustainable-products (Accessed: 18 December 2020).

GreenGate (2020) *Eco-friendly Catering Disposables | Green Gate Bio Packaging*. Available at: https://shop.biogreengate.com/ (Accessed: 18 December 2020).

Hansen, N. M. L. and Plackett, D. (2008) ‘Sustainable films and coatings from hemicelluloses: A review’, *Biomacromolecules*. American Chemical Society, 9(6), pp. 1493–1505. doi: 10.1021/bm800053z.

Haugaard, V. K. *et al.* (2000) *Biobased Packaging Materials for the Food Industry Status and Perspectives*. Edited by C. J. Weber. KVL Dept. of Dairy and Food Science.

Holman, J. P. (2010) *Heat Transfer*. 10th edn. McGraw-Hill. doi: 10.1016/b978-1-933762-24-1.50019-x.

Kale, M. S. *et al.* (2018) 'Molecular and functional properties of a xylanase hydrolysate of corn bran arabinoxylan', *Carbohydrate Polymers*. Elsevier, 181(August 2017), pp. 119–123. doi: 10.1016/j.carbpol.2017.10.008.

Kayserilioğlu, B. Ş. *et al.* (2003) 'Use of xylan, an agricultural by-product, in wheat gluten based biodegradable films: Mechanical, solubility and water vapor transfer rate properties', *Bioresource Technology*, 87(3), pp. 239–246. doi: 10.1016/S0960-8524(02)00258-4.

Li, Q. *et al.* (2020) 'The Application of Polysaccharides and Their Derivatives in Pigment, Barrier, and Functional Paper Coatings', *Polymers*, 12(8). doi: doi:10.3390/polym12081837.

LivBar (2020) *LivBar | Organic Superfood Energy Bars*. Available at: https://livbar.com/ (Accessed: 18 December 2020).

Ly, B. C. K. *et al.* (2020) 'Research Techniques Made Simple: Cutaneous Colorimetry: A Reliable Technique for Objective Skin Color Measurement', *Journal of Investigative Dermatology*. The Authors, 140(1), pp. 3-12.e1. doi: 10.1016/j.jid.2019.11.003.

Mendez-Encinas, M. A. *et al.* (2018) 'Ferulated Arabinoxylans and Their Gels: Functional Properties and Potential Application as Antioxidant and Anticancer Agent', *Oxidative Medicine and Cellular Longevity*, 2018. doi: 10.1155/2018/2314759.

Mikkonen, K. S. *et al.* (2009) 'Films from oat spelt arabinoxylan plasticized with glycerol and sorbitol', *Journal of Applied Polymer Science*, 114(1), pp. 457–466. doi: 10.1002/app.30513.

Mohanty, K. and Purkait, M. K. (2011) *Membrane technologies and applications*, *Membrane Technologies and Applications*. doi: 10.1002/9781118359686.

Mulder, M. (1997) *Basic Principles of Membrane Technology*. 2nd Editio. Kluwer Academic Publishers.

Paz-Samaniego, R. *et al.* (2015) 'Gelation of Arabinoxylans from Maize Wastewater — Effect of Alkaline Hydrolysis Conditions on the Gel Rheology and Microstructure', *Wastewater Treatment Engineering*. doi: 10.5772/61022.

Pereira, P. H. F. *et al.* (2017) 'Wheat straw hemicelluloses added with cellulose nanocrystals and citric acid. Effect on film physical properties', *Carbohydrate Polymers*. Elsevier Ltd., 164, pp. 317–324. doi: 10.1016/j.carbpol.2017.02.019.

Péroval, C. *et al.* (2002) 'Edible arabinoxylan-based films. 1. Effects of lipid type on water vapor permeability, film structure, and other physical characteristics', *Journal of Agricultural and Food Chemistry*, 50(14), pp. 3977–3983. doi: 10.1021/jf0116449.

Piergiovanni, L. and Limbo, S. (2013) *Food Packaging Materials*, *Springer*. doi: 10.1007/978-3-319-24732-8.

Preedy, V. R. and Watson, R. R. (2019) *Flour and Breads and Their Fortification in Health and Disease Prevention*. 2nd Editio. Edited by V. R. Preedy and R. R. Watson. Elsevier. Available at: http://repositorio.unan.edu.ni/2986/1/5624.pdf.

PubChem (2020a) *Citric acid*. Available at: https://pubchem.ncbi.nlm.nih.gov/compound/Citric-acid (Accessed: 28 November 2020).

PubChem (2020b) *Maleic acid*. Available at: https://pubchem.ncbi.nlm.nih.gov/compound/Maleic-acid (Accessed: 28 November 2020).

PubChem (2020c) *Malonic acid*. Available at: https://pubchem.ncbi.nlm.nih.gov/compound/Malonic-acid (Accessed: 28 November 2020).

PubChem (2020d) *Oxalic acid*. Available at: https://pubchem.ncbi.nlm.nih.gov/compound/Oxalic-acid (Accessed: 28 November 2020).

PubChem (2020e) *Succinic acid*. Available at: https://pubchem.ncbi.nlm.nih.gov/compound/Succinic-acid (Accessed: 28 November 2020).

Qin, M. *et al.* (2019) 'Comparison of energy consumption in desalination by capacitive deionization and reverse osmosis', *Desalination*. Elsevier, 455(November 2018), pp. 100–114. doi: 10.1016/j.desal.2019.01.003.

Rose, D. J., Inglett, G. E. and Liu, S. X. (2010) 'Utilisation of corn (Zea mays) bran and corn fiber in the production of food components', *Journal of the Science of Food and Agriculture*, 90(6), pp. 915–924. doi: 10.1002/jsfa.3915.

Scott, K. (1998) *Handbook of Industrial Membranes*. Elsevier.

Serra, M. *et al.* (2020) 'Purification of arabinoxylans from corn fiber and preparation of bioactive films for food packaging', *Membranes*, 10(5), pp. 1–22. doi: 10.3390/membranes10050095.

Sessa, D. J. *et al.* (2003) 'Improved methods for decolorizing corn zein', *Industrial Crops and Products*, 18(1), pp. 55–65. doi: 10.1016/S0926-6690(03)00033-5.

Sessa, D. J. and Palmquist, D. E. (2009) 'Decolorization/deodorization of zein via activated carbons and molecular sieves', *Industrial Crops and Products*, 30(1), pp. 162–164. doi: 10.1016/j.indcrop.2008.12.008.

Shao, H. *et al.* (2019) 'Facile and green preparation of hemicellulose-based film with elevated hydrophobicity: Via cross-linking with citric acid', *RSC Advances*, 9(5), pp. 2395–2401. doi: 10.1039/c8ra09937e.

Shao, L. *et al.* (2020) 'Decolorization affects the structural characteristics and antioxidant activity of polysaccharides from Thesium chinense Turcz: Comparison of activated carbon and hydrogen peroxide decolorization', *International Journal of Biological Macromolecules*. Elsevier B.V., 155, pp. 1084–1091. doi: 10.1016/j.ijbiomac.2019.11.074.

Shi, L. (2016) 'Bioactivities, isolation and purification methods of polysaccharides from natural products: A review', *International Journal of Biological Macromolecules*. Elsevier B.V., 92, pp. 37–48. doi: 10.1016/j.ijbiomac.2016.06.100.

Stoklosa, R. J. *et al.* (2019) 'Evaluation of arabinoxylan isolated from sorghum bran, biomass, and bagasse for film formation', *Carbohydrate Polymers*. Elsevier, 213(March), pp. 382–392. doi: 10.1016/j.carbpol.2019.03.018.

Takht Ravanchi, M., Kaghazchi, T. and Kargari, A. (2009) 'Application of membrane separation processes in petrochemical industry: a review', *Desalination*. Elsevier B.V., 235(1–3), pp. 199–244. doi: 10.1016/j.desal.2007.10.042.

Vegware (2020) *Vegware - Our materials*. Available at: https://www.vegware.com/uk/page/our-materials/#materials-plants (Accessed: 18 December 2020).

Vieira, M. G. A. *et al.* (2011) 'Natural-based plasticizers and biopolymer films: A review', *European Polymer Journal*. Elsevier Ltd, 47(3), pp. 254–263. doi: 10.1016/j.eurpolymj.2010.12.011.

Xiang, Z. *et al.* (2016) 'Glutaraldehyde crosslinking of arabinoxylan produced from corn ethanol residuals', *Cellulose*. Springer Netherlands, 23(1), pp. 307–321. doi: 10.1007/s10570-015-0828-3.

Yan, J. *et al.* (2019) 'Rheological and emulsifying properties of arabinoxylans from various cereal brans', *Journal of Cereal Science*. Elsevier, 90(33), p. 102844. doi: 10.1016/j.jcs.2019.102844.

Yang, Y. C. *et al.* (2019) 'Fabrication of antimicrobial composite films based on xylan from pulping process for food packaging', *International Journal of Biological Macromolecules*. Elsevier B.V., 134, pp. 122–130. doi: 10.1016/j.ijbiomac.2019.05.021.

Zhang, Z., Smith, C. and Li, W. (2014) 'Extraction and modification technology of arabinoxylans from cereal by-products: A critical review', *Food Research International*. Elsevier Ltd, 65(PC), pp. 423–436. doi: 10.1016/j.foodres.2014.05.068.

Zhurlova, O. D. (2017) 'The Current Trends and Future Perspectives of Arabinoxylans

Prebiotics Research: a Review', *Зернові Продукти І Комбікорми*, 17(4), pp. 4–11. doi: 10.15673/gpmf.v17i4.760.

Zoldners, J. and Kiseleva, T. (2013) 'Modification of hemicelluloses with polycarboxylic acids', *Holzforschung*, 67(5), pp. 567–571. doi: 10.1515/hf-2012-0183.

7. Appendix

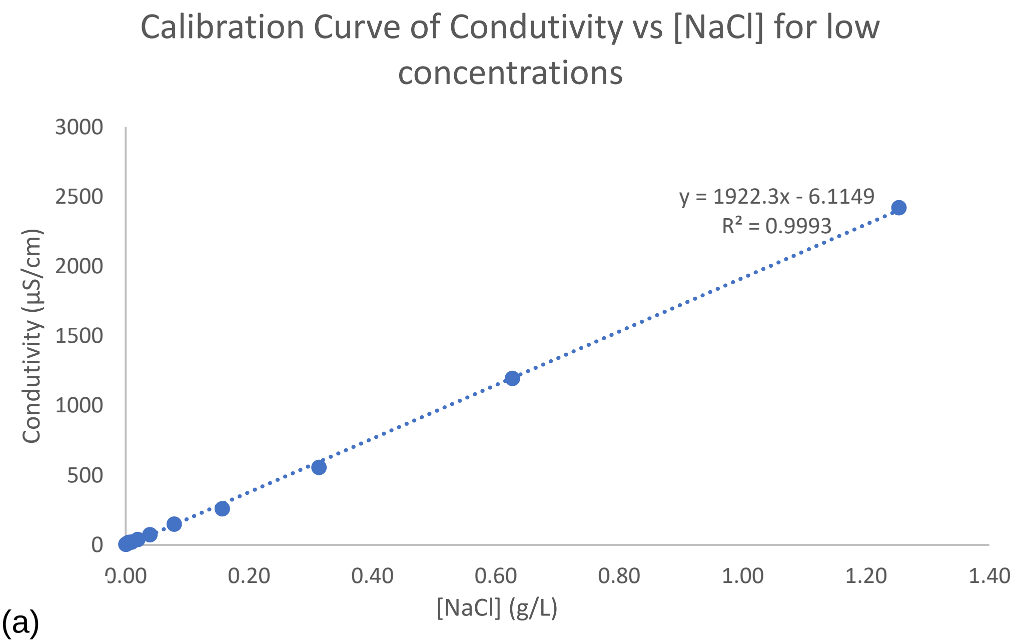

(a)

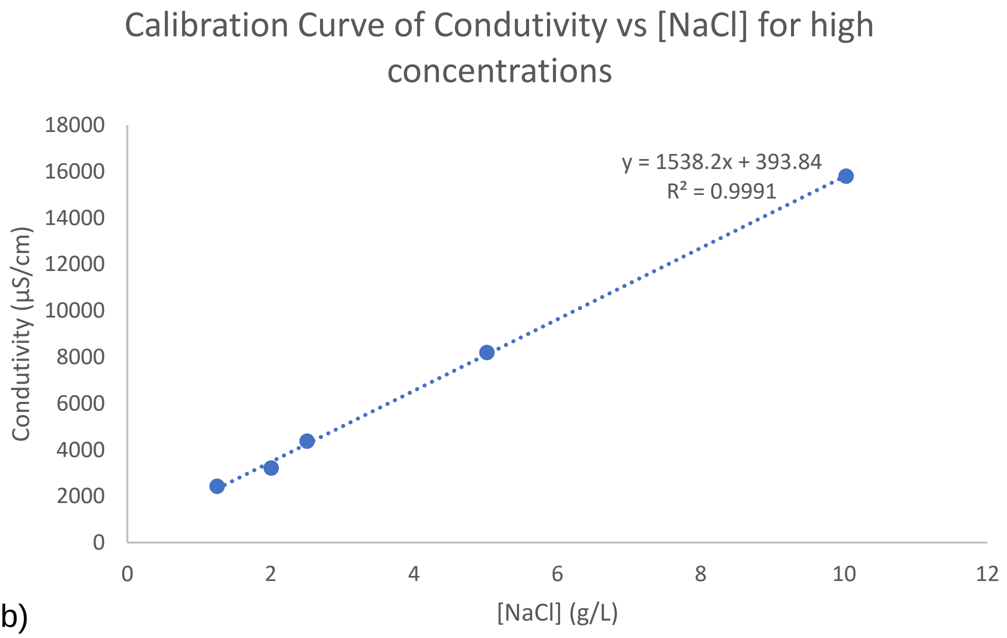

(b)

Figure A.1: Calibration curve of conductivity in function of concentration of NaCl (a)for lower concentrations (b)for higher concentrations

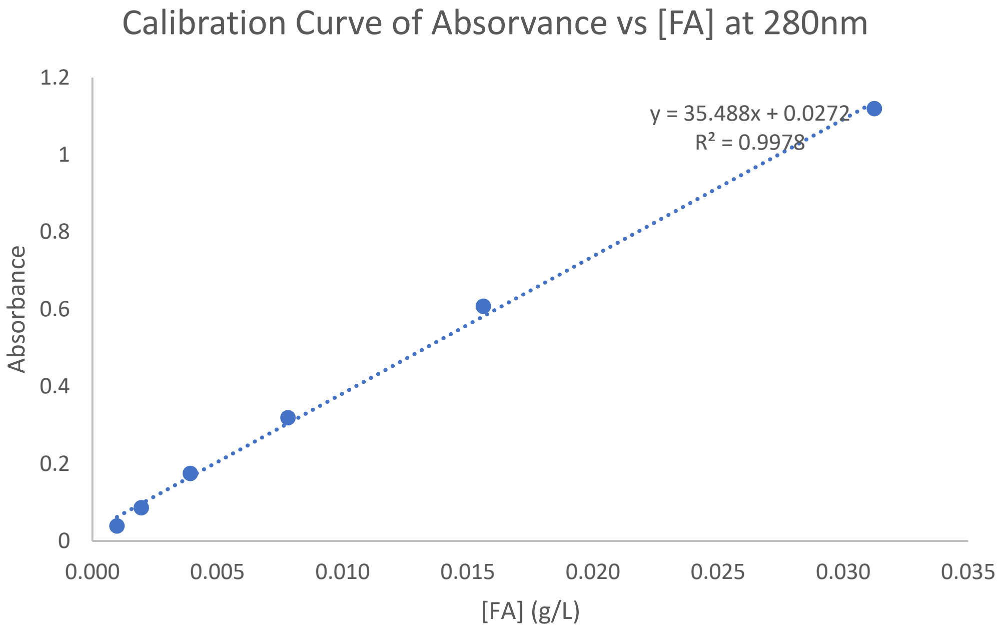

Figure A.2: Calibration curve of absorbance at 280nm in function of concentration of FA

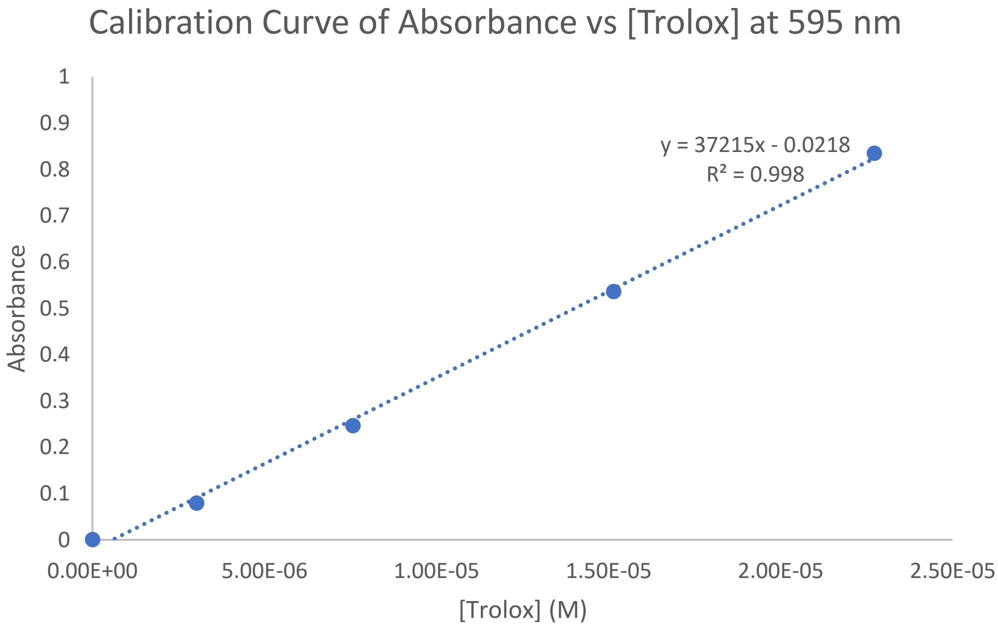

Figure A.3: Calibration curve of absorbance at 595nm in function of concentration of Trolox

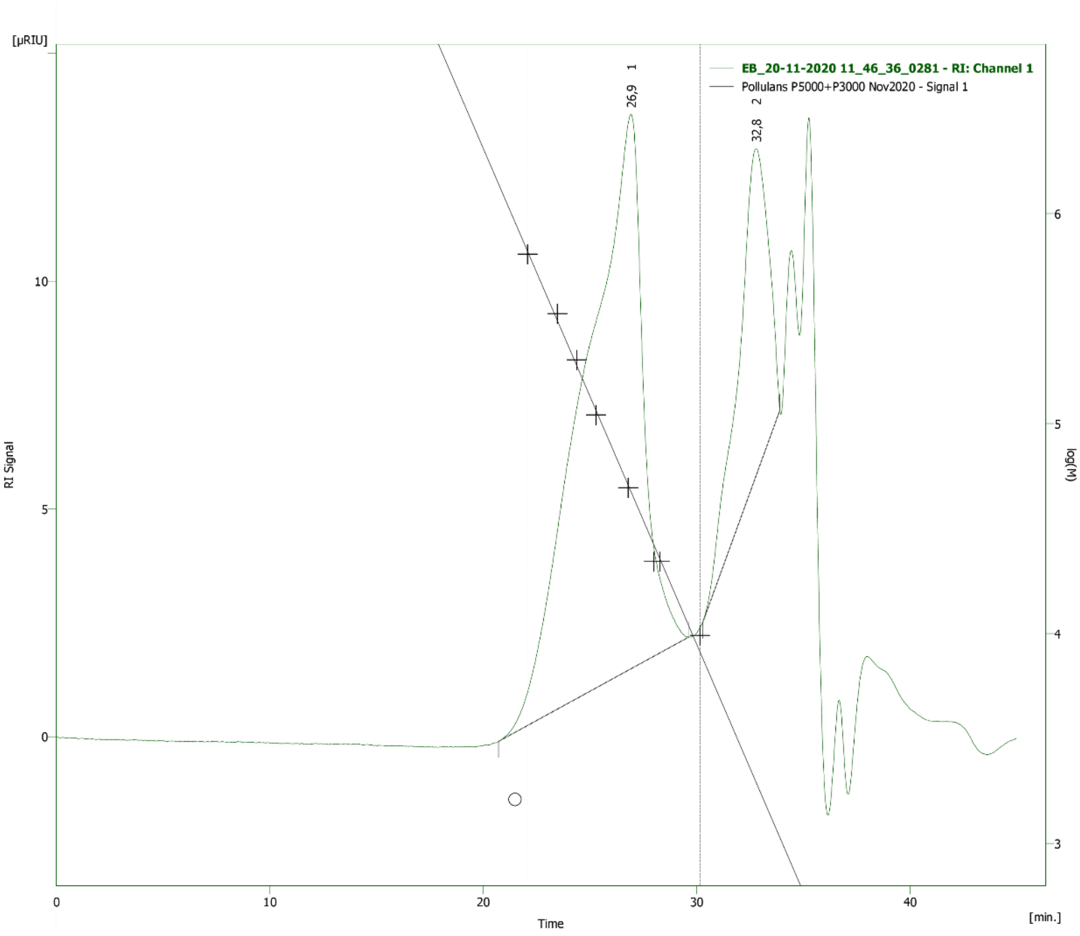

Figure A.4: Chromatogram of raw extract

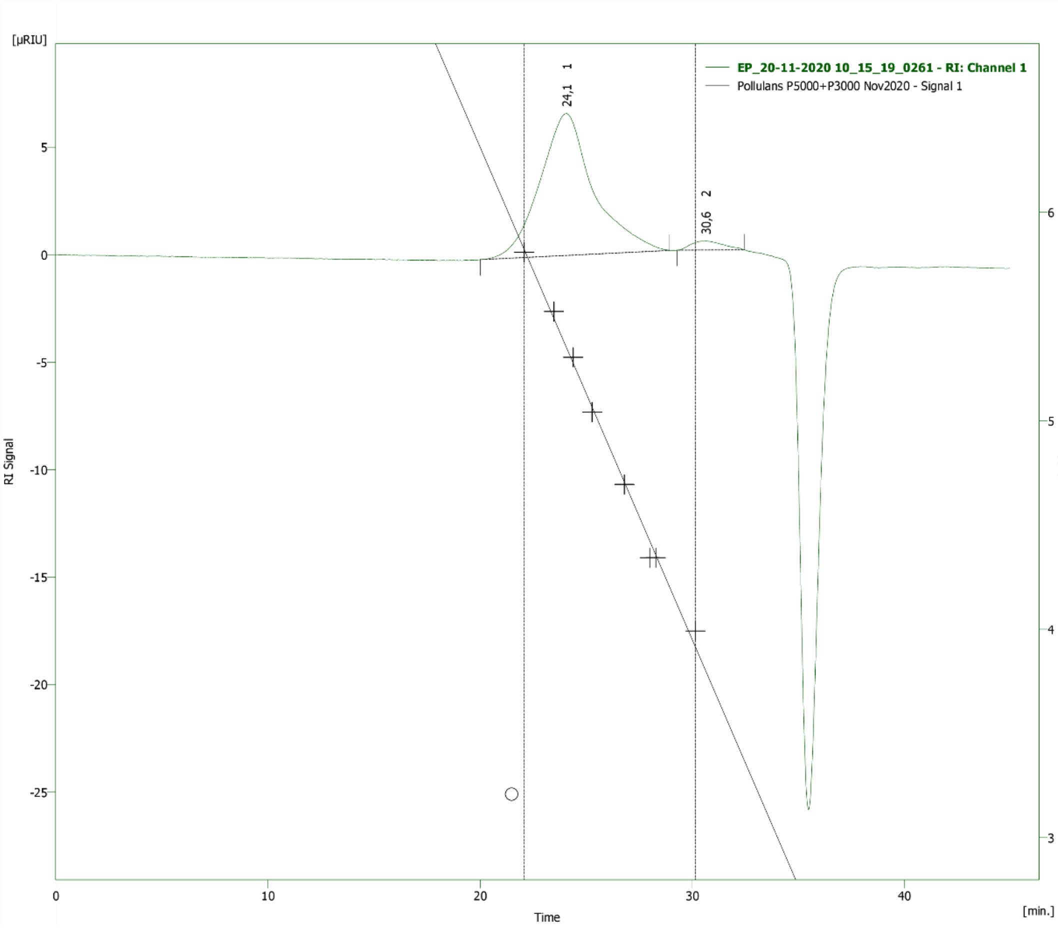

Figure A.5:Chromatogram of purified extract

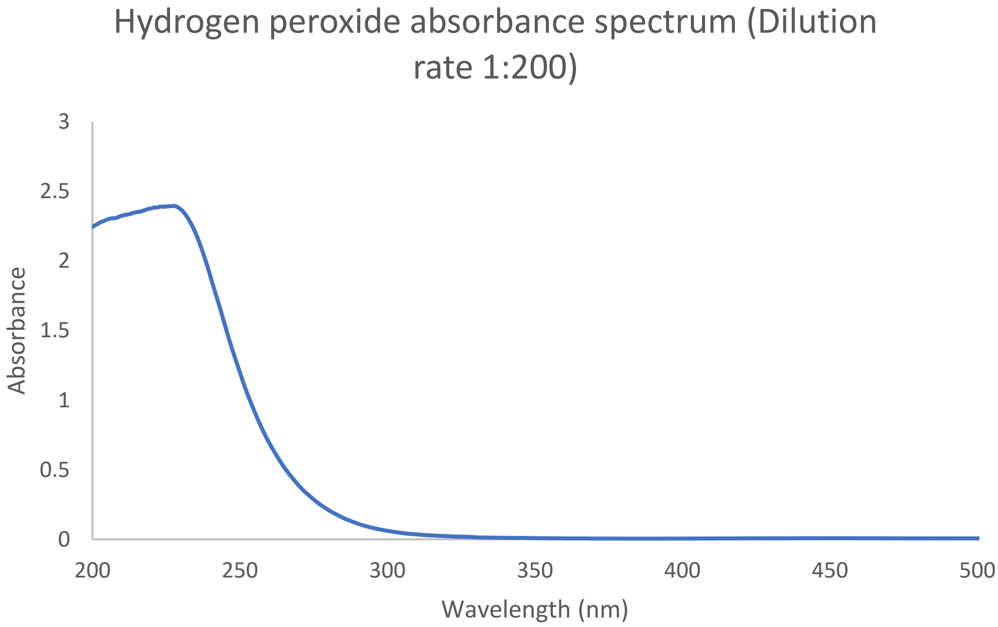

Figure A.6: Absorbance spectrum of hydrogen peroxide in a dilution rate of 1:200